

TABLE OF CONTENTS

A) Procedures and Protocols:

1. Materials and instruments	S4
2. Synthesis, characterisation data, and solubility	S5
3. HPLC studies	S6
4. LC-MS experiments	S6
5. Pt content by ICP-MS	S7
6. DNA thermal denaturation experiments	S7
7. Calculation of singlet oxygen quantum yields	S7
8. DFT and TDDFT calculations	S8
9. MTT assay	S8
10. Cellular ROS quantification by DCFDA assay	S8
11. Cellular apoptosis assay	S9
12. Confocal imaging	S9
13. Cell fractionation	S10

B) Graphics:

Figure S1. Synthetic scheme	S11
Figures S2-S7. NMR and mass spectra of IR797-acac and complex 1	S12-S15
Figure S8. HPLC chromatograms for IR797-acac and complex 1	S16
Figure S9. Absorption and emission spectra of IR797-acac and complex 1	S17
Figure S10. Absorption spectra of IR797-acac in light	S17
Figure S11. Absorption spectra showing stability in dark	S18
Figures S12-S17. LC-MS traces of the photoproducts	S19-S24
Figure S18. Stability and plot of ion counts vs irradiation time	S25

Figure S19-S20. NMR spectra showing photodecomposition	S26-S27
Figure S21. Absorption and emission spectra of 1 in absence of oxygen	S28
Figure S22. Scheme showing photodegradation of IR797-acac	S29
Figure S23. Mass spectra of Pt-pyridine adducts	S30
Figure S24. DNA binding plots	S31
Figure S25. DPBF studies for singlet oxygen detection	S32
Figure S26. DFT optimized excited triplet state of complex 1	S33
Figure S27. DFT optimized structures of P1a and P1b	S34
Figures S28-S31. MTT assay curves in different cell lines	S35-38
Figure S32. ESI-MS of mixture of cisplatin and IR797-acac	S39
Figure S33. DCFDA assay showing ROS generation in cells	S40
Figure S34. AnnexinV-FITC/ PI assay showing apoptosis in cells	S41
Figure S35. Confocal images	S41
<i>C) Tables:</i>	
Table S1. Spectroscopic data and important parameters of 1 and IR797-acac	S42
Table S2. Amounts of Pt in isolated ct-DNA	S42
Table S3. Optimized coordinates of complex 1	S43
Table S4. TDDFT predicted transitions of complex 1	S44
Table S5. Parameters for g.s and e.s. of complex 1	S45
Table S6. TDDFT predicted singlet transitions in P1a and P1b	S46
Table S7. IC ₅₀ values of the compounds in the investigated cell lines	S47
Table S8. Cellular uptake of Pt in cancer cells	S47
<i>D) References</i>	S48

A) Procedures and Protocols:

1. Materials and instruments: All reactions were performed in an inert atmosphere using dry solvents and oven-dried glassware. The reactions were carried out in light-protected hoods using Al foil-wrapped glassware. All chemicals were purchased from commercial sources (Sigma Aldrich, Fisher Scientific, VWR, TCI America and Life Technologies) and were used as received. ctDNA was purchased from Sigma-Aldrich (catalog no: D1501). Complex **2** was prepared by known protocols and the characterization data matched with literature reports.^[S11] ¹H and ¹³C NMR spectra were recorded using either a 400 MHz Bruker Avance or a 300 MHz Varian spectrometer. ¹H NMR data was reported with the following parameters: chemical shift (δ), coupling constant (J) and integration values. ¹³C NMR data was reported in chemical shifts. Electrospray ionization (ESI-MS) and high-resolution liquid chromatography mass spectral (LC-MS) analyses were performed with “Thermo Finnigan LCQ deca XP max” mass spectrometer in positive mode ionization. Absorption and fluorescence measurements were carried out using Varian Cary Eclipse and Agilent spectrophotometers. Platinum content was measured by inductively coupled plasma mass spectrometric (ICP-MS) method using Varian ICP 820-MS instrument. High performance liquid chromatography (HPLC) purification was carried out using a Shimadzu Prominence system using Vydac (218TP C18 5 μ) column using acetonitrile and water as eluents (10-100% gradient) and was monitored at 770 and 430 nm. Excited state lifetimes were measured using Zeiss 780 multiphoton microscopy equipped with a Becker & Hickl FLIM hybrid detector (HPM-100-40). The decay curves were obtained using a bi-exponential fitting model with software SPCI. All experiments were performed using HPLC purified samples which were aliquoted in DMSO and stored at -80 °C. MTT assay readings were taken using a BioTek Synergy H1 hybrid 96-well plate reader. Canto - BD FACSCanto™ II Analyzer instrument, equipped with BD FACS carousel loader and 2 lasers (blue: 488 nm, red: 633 nm) helped with FACS (Fluorescence activated cell sorting) data recording. FACSDIVA and FCSExpress 5 flow software were used for data analysis. Confocal images were acquired using LSM710 Zeiss instrument (63X magnification using oil-immersion objective). Image processing was conducted with Zen and ImageJ software. The experiments denoted as “dark” were carried out in Al foil-wrapped light protected conditions, while the experiments requiring “light” exposure was carried out using commercially available LED bulbs (720-740 nm, RapidLED, Solderless Cree XP-E Far Red Led) with an average output

of $(3.5 \pm 1.5) \text{ mW.cm}^{-2}$. The intensity measurement of the LED source was done with a Thorlabs PM100 optical power and energy meter.

2. Synthesis, characterization data, and solubility

Synthesis of IR797-acac

IR797 chloride (250 mg, 0.49 mmol), acetylacetone (245 μL , 2.45 mmol) and N,N-diisopropylethylamine (90 μL , 0.49 mmol) were dissolved in acetonitrile (10 mL) in a sealed vial. The dark green colored solution was heated at 70°C on a microwave apparatus (Discover, CEM, 60 W) for 15 mins. The progress of the reaction was monitored via TLC and stopped only after full consumption of the starting dye. The reaction mixture was allowed to cool down to room temperature and dichloromethane (50 mL) was added. The organic layer was washed using saturated sodium bicarbonate solution (2 x 10 mL), dried over anhydrous sodium sulfate, filtered, and evaporated using a rotavac. The crude material was subjected to column chromatography using ethyl acetate (100%) and dichloromethane-methanol eluents (0-10%) to yield pure product, IR797-acac (150 mg, 50% yield). $^1\text{H NMR}$ (400 MHz, CDCl_3): δ (ppm) = 7.43-7.36 (m, 4H), 7.31 (d, $J = 7.4 \text{ Hz}$, 2H), 7.21 (t, $J_1 = J_2 = 7.2 \text{ Hz}$, 2H), 7.11 (d, $J = 8.0 \text{ Hz}$, 2H), 6.20 (d, $J = 14 \text{ Hz}$, 2H), 3.74 (s, 6H), 3.15 (s, 4H), 2.00 (s, 6H), 1.58 (s, 12H). $^{13}\text{C NMR}$ (100 MHz, CDCl_3): δ (ppm) = 191.42, 170.78, 144.66, 142.96, 140.71, 137.40, 128.80, 124.99, 122.04, 110.04, 103.39, 48.82, 32.53, 28.42, 23.60. ESI-MS in MeCN: m/z (expected) = 533.33, m/z (observed) = 533.32 $[\text{M} - \text{Cl}]^+$ (100%). The compound was readily soluble in polar solvents such as acetonitrile, methanol, chloroform, dichloromethane, dimethylsulfoxide and dimethylformamide.

Synthesis of IR797-Platin (1)

Cisplatin (25 mg, 0.08 mmol) and silver nitrate (27 mg, 0.1625 mmol) were dissolved in dimethylformamide (2 mL) and stirred at room temperature in the dark. After 24 h, the solution was centrifuged and filtered to remove the white precipitate (silver chloride). To this pale yellow colored filtrate, IR797acac (50 mg, 0.08 mmol) and N,N-diisopropylethylamine (100 μL) was added. The solution was stirred at room temperature for 6 h in the dark. The solvent was removed using a rotavac to obtain a green sticky material which was dissolved in 10 mL of methanol and precipitated by slowly adding ice-cold diethyl ether (100 mL) with continuous stirring. The solution was centrifuged to obtain a green precipitate. This dissolving-precipitating protocol was

repeated to isolate a crude product, which was further subjected to HPLC chromatographic separation to obtain IR797-Platin, **1** as pure product (yield = 20 mg, 0.02 mmol, 25%). ¹H NMR (400 MHz, MeOD-*d*₄) : δ (ppm) = 7.45 (d, J = 12 Hz, 2H), 7.38-7.32 (m, 4H), 7.20-7.16 (m, 4H), 6.01 (d, J = 14 Hz, 2H), 3.53 (s, 6H), 2.93 (s, 4H), 1.67 (s, 6H), 1.51 (s, 12H). ¹³C NMR (100 MHz, MeOD-*d*₄): δ (ppm) = 190.73, 171.47, 143.05, 140.84, 137.64, 136.57, 128.43, 124.88, 121.93, 110.42, 101.87, 42.54, 30.15, 26.80, 21.79. ESI-MS in MeOH: *m/z* (expected) = 380.66, *m/z* (observed) = 380.66 [M – NO₃– Cl]²⁺ (100%). The complex was soluble in polar solvents such as acetonitrile, methanol, dimethylsulfoxide and dimethylformamide.

3. High performance liquid chromatography: For verifying purity, samples (25 μ l in 2.5% DMSO-H₂O) were loaded on an analytical C18 column and gradient was maintained at 10-100 percent of MeCN-H₂O from 10-50 min. The absorbance was measured at different wavelengths within the range of 200-800 nm. For photolysis experiments, solution of **1** (30 μ l of 100 nM in 0.1% of DMSO-PBS, irradiated for 1 min) was injected on the column and eluted using the same gradient as above. The photoproducts were observed at 770 nm and/or 430 nm and assigned by recording the mass spectra of the collected fractions.

4. Liquid-chromatography mass spectral experiments: Solutions of **1** and IR797-acac (100 nM in 0.1 % DMSO-PBS) were used to carry out LC-MS studies. Samples were injected on a self-packed fused silica (polymicro technologies) trap column (360 micron o.d. X 100 micron i.d.) with a Kasil frit packed with 5-15 micron irregular phenyl C-18 YMC packing. The trap column is connected to an analytical column (360 micron X 50 micron) with a fritted tip at 5 micron or less (New Objective) packed with 5 μ m phenyl C-18 YMC packing. Compounds were initially trapped and then eluted into a Thermo Finnigan LCQ deca XP max mass spectrometer (Thermo Scientific) with an acetonitrile gradient from 0 % to 80 % over 5 minutes at a flow rate of between 50-150 nL/min. The mass spectrometer scanned in the following sequence: a MS scan from mass 100-1000 *m/z* is collected, followed by a zoom scan to verify charge state, then a MS/MS scan to validate structure and placed on an exclusion list for 1 min. Integration of the extracted ion chromatogram yielded its relative abundance in the samples.

5. DNA bound Pt content: A 1X-PBS solution containing ctDNA (500 μM) and **1** (50 μM in 0.1% DMSO-PBS) was irradiated with near-IR light (720-740 nm) for 15, 30 and 60 mins. Another identical set was incubated in dark for comparison. After treatment, the DNA was precipitated from the solutions using 10 mL of cooled ethanol, vortexed, and collected by centrifugation.^[S2] The precipitate was washed twice with cooled ethanol (5 mL) to remove soluble platinum complexes. The white fibrous precipitate was dissolved using 200 μl of conc. HNO_3 for 12 h and diluted with distilled water to 2% HNO_3 -water solutions. Platinum content was measured by ICP-MS instrument. Untreated samples (DNA alone, complex alone) were kept for control. Platinum standards were made by dissolving K_2PtCl_4 in 98% aq. HNO_3 and used for calibration. The data along with the deviation is reported based on experiments performed in duplicate.

6. DNA thermal denaturation experiments: The DNA thermal denaturation experiments were performed by monitoring the absorption intensity of ct-DNA (200 μM) at 260 nm at increasing temperatures (from 40 to 90 $^\circ\text{C}$), both in the absence and presence of complex **1** and IR797-acac (20 μM in 1% DMSO-DPBS solutions, pH = 7.2). The experiments were performed using Agilent UV-visible spectrophotometer connected to a Peltier thermostat for temperature control. Data was recorded with increasing the temperature of the solution by 1.0 $^\circ\text{C}$ per min. The derivative of the melting plots gave the DNA melting temperature (T_m) of the ct-DNA. Ethidium bromide (20 μM) as a standard intercalator was used for comparison.

7. Calculation of singlet oxygen quantum yields by DPBF method: The singlet oxygen quantum yields were obtained following standard literature methods.^[S3] To improve the stability of DPBF, the singlet oxygen quenching experiments were carried out in aerated DMF solutions. The concentration of DPBF was adjusted so as to obtain an absorbance of ~ 1 unit at 415 nm. To this solution, **1** or IR797-acac was added in concentrations so that the absorbance at ~ 790 nm was in the range 0.1-0.3 units. This ratio of DPBF and compounds ensured minimum self-quenching of singlet oxygen by the dyes. Light exposure was performed with 720-740 nm LEDs for different time intervals. The relative quantum yields of singlet oxygen generation (ϕ_Δ) were calculated by using the equation: $\phi_\Delta = \phi_\Delta^{\text{ref}} (k/k^{\text{ref}})(I_a^{\text{ref}}/I_a)$, in which ϕ_Δ^{ref} is the singlet oxygen quantum yield for the standard (methylene blue, $\phi_\Delta = 0.52$), k and k^{ref} are the photobleaching rate constants of DPBF, and I_a and I_a^{ref} are the absorption intensities (790 nm) of the compound and standard.

8. Theoretical calculations: The coordinates for cationic **1** and the dioxetane intermediates (P1a and P1b) were obtained from Chemcraft software by drawing the molecules. These coordinates were then optimized by density functional theory (DFT) calculations using B3LYP/ LanL2DZ (for Pt atom) and 6-31+G (for C, H, N and O) and executed with G09 systems.^[S4] These energy-minimized structures were computed using linear response time dependent density functional theory (TDDFT) to evaluate the electronic transitions and the spin density of the orbitals.

9. MTT assay: Cytotoxic profiles of the compounds were assessed in the following cell lines (passage number not exceeding 15): MCF-7 (human breast cancer) C-33 A (human cervical carcinoma) and HEK293T (transformed human kidney). Around 6000 cells were seeded in 96 well transparent flat-bottom tissue-culture plate in 200 μ l of Dulbecco's Modified Eagle Medium (DMEM) containing 10% FBS (Fetal Bovine Serum) and were incubated for 24 h at 37 °C and 5% CO₂. We performed an initial control experiment with vehicle alone (0.1 % DMSO-DMEM) on cells with different dosages of near-IR light and compared it to unexposed counterparts. The cells were unharmed by light and vehicle alone up to 45 min of photoirradiation. Cells were treated with various concentrations of **1**, **2**, IR797-acac, cisplatin and an equimolar mixture of IR797-acac and cisplatin in 0.1 % DMSO-DMEM for 4 h or 48 h in the dark. One such plate was exposed to near-IR light for 45 min in phenol-red free DMEM (200 μ l) and room temperature was maintained using a cooling system. Another identical plate was kept in dark. The plates were incubated for another 24 h in dark. Finally, MTT [3-(4,5-dimethylthiazole-2-yl)-2,5-diphenyltetrazolium bromide] (25 μ l of 5 mg/ml solution in PBS) was added and incubated for 3-4 h.^[S5] The absorbance of the precipitated formazan was recorded at 550 nm in DMSO. Cells treated with 0.1 % DMSO-DMEM was kept as controls which represented 100% viability. The half-growth inhibitory concentration (IC₅₀) values were calculated by nonlinear regression analysis using GraphPad Prism5. The data is represented from two independent set of experiments, each of which was performed in triplicate.

10. ROS detection: Reactive oxygen species (ROS) can be quantified by measuring fluorescence intensity at 525 nm of DCF (2,7-dichlorofluorescein) which is an oxidized product of DCFDA, the diacetate analog of DCF.^[S6] Human cervical cancer cells, C-33 A (seeding density $\sim 10^5$ cells) were plated in 6-well plates and allowed to attach for 24 h. Cells were treated with complex **1** (1 μ M in 0.05% DMSO-DMEM) for 4 h in dark. DMEM was replaced with phenol-red free DMEM

and cells were either irradiated (near-IR light, 45 min) or kept in dark. Cells were then treated with 0.05% trypsin for 10 min and centrifuged. The pellets were re-suspended in PBS and incubated with 1 μ M DCFDA 15 min at room temperature in dark. Unstained and stained cells treated only with 0.05% DMSO were kept as control. The data were collected by FACS instrument and represented as histograms or bar diagrams from experiments done in duplicate.

11. Apoptosis assay: Early apoptotic cells show selective cellular internalization of AnnexinV-fluorescein isothiocyanate (FITC) dye and late apoptotic/ necrotic cells are permeable to both AnnexinV-FITC and propidium iodide (PI). Dead cells are selectively stained by PI. Therefore, measuring the uptake of the dyes can quantify the amount of the cells showing an apoptotic mode of cell death.^[S7] Human cervical cancer cells, C-33 A (~ 10^5 cells) were incubated with **1** (1 μ M in 0.05% DMSO-DMEM) for 4 h in dark. Cells were either irradiated with near-IR light for 45 min or kept in the dark in phenol-red free DMEM. Cells were incubated overnight in 10%-DMEM-FBS, after which they were precipitated by 0.05% trypsin treatment for 10 min and collected by subsequent centrifugation. Annexin V-FITC apoptosis detection kit (Sigma Aldrich, APOAF-20T ST) was used for this assay. 500 μ L of 1X binding buffer was used to re-suspend the cell pellets which were then stained using Annexin V-FITC (1 μ L) and PI (0.5 μ L) for 10 min in dark. The fluorescence intensities were determined with FACS instrument. Cells treated with 0.05% DMSO only were used for calibrating unstained and stained cells (PI alone, AnnexinV-FITC alone, both PI and AnnexinV-FITC). The data is obtained from experiments performed in duplicate and represented as percentage population of early and late apoptotic cells.

12. Confocal microscopic experiments: Confocal microscopic images were recorded using LSM710 Zeiss instrument at 63X magnification. Human cervical cancer cells, C-33 A were plated on cover slips in a 12-well tissue-culture plate and allowed to attach for 24 h. They were treated with complex **1** (1 μ M in 0.05% DMSO) for 4 h in the dark. The cells were washed with PBS and treated with 4,6-diamidino-2-phenylindole, dihydrochloride (DAPI, nuclear stain, 300 nM), Mito-Tracker[®] Green (50 nM) and Lyso Tracker[®] Red DND-99 (50 nM) in a stepwise protocol and washed properly to avoid non-specific staining. The cover slips were mounted on slides with a drop of AntifadeGold reagent and attached by coating the periphery using transparent nail-enamel. Cells treated with 0.05% of DMSO and stained with the dyes alone were used as control for

parameter optimization and to avoid auto-fluorescence and false background signals. Multiple images were taken from duplicate samples to confirm the homogeneity in obtained results.

13. Pt Content in whole cells and nuclear/ cytosolic fractions: Approximately, 10^6 C-33 A cells were plated in 100 mm tissue culture treated petri dishes and allowed to attach for 24 h. Cells were then treated with complex **1** ($50 \mu\text{M}$ in 0.1% DMSO-DMEM) and incubated for 4 h in dark. Dishes were either exposed to light (720-740 nm, 15 min) or kept in dark. The cells were then allowed to incubate in dark for an additional 6 h. The cells were washed with PBS and collected as pellets by centrifugation. The untreated controls were utilized to determine the total number of cells by trypan blue method (deviation is within $\pm 10\%$). For estimation of Pt in whole cell, the pellets were simply dissolved overnight in conc. HNO_3 . The cellular fractionation was done using Thermo Fisher Scientific NE-PERTM nuclear and cytoplasmic extraction reagents following the protocol with CER-I and CER-II buffer only as specified in the kit. The obtained nuclear and cytosolic fractions were dissolved overnight in conc. HNO_3 and diluted to 98% aq. HNO_3 solutions and measured for Pt content by ICP-MS instrument along with standards.

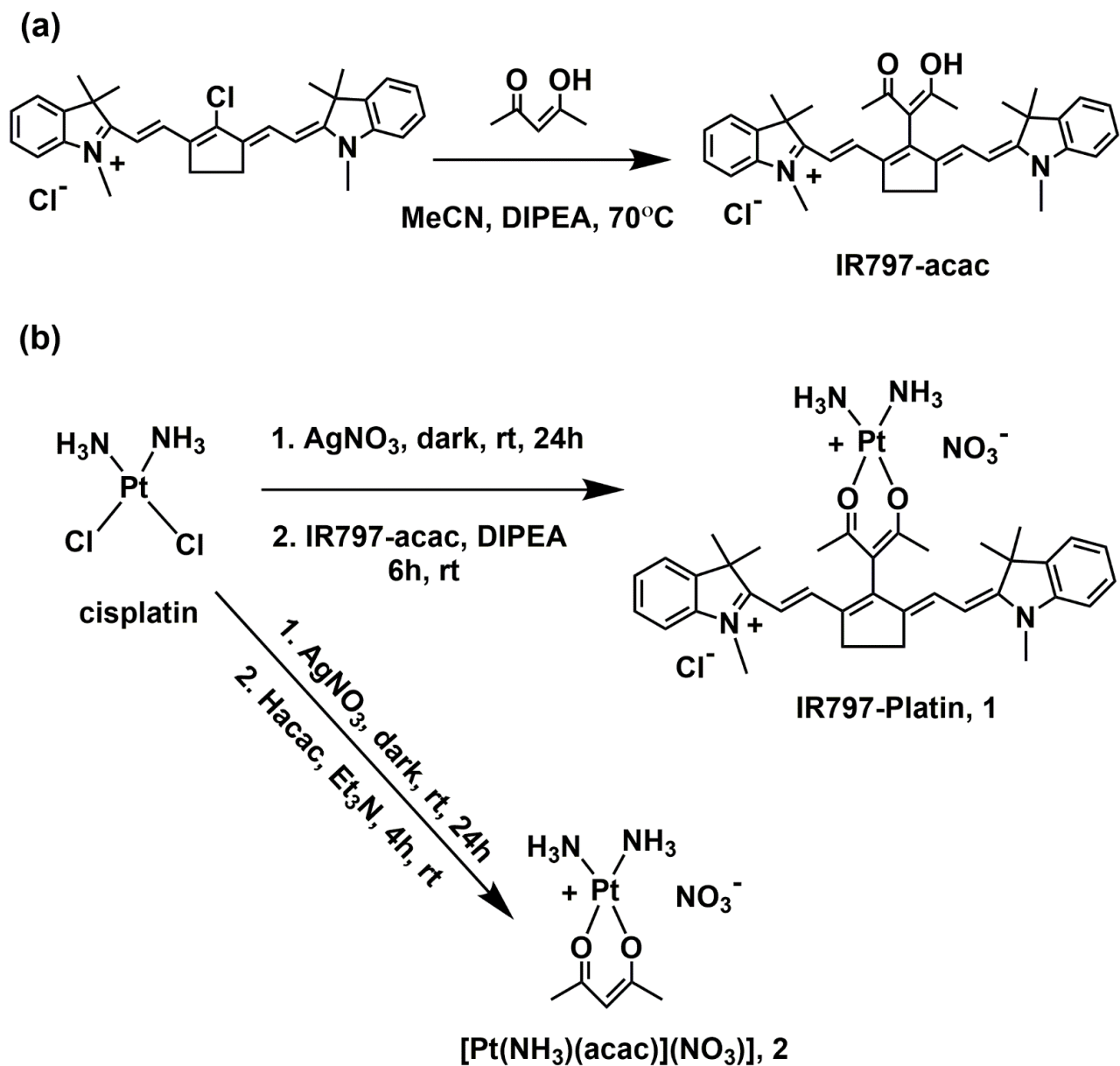


Figure S1. Scheme showing synthesis of IR797-acac, complexes **1** and **2**.

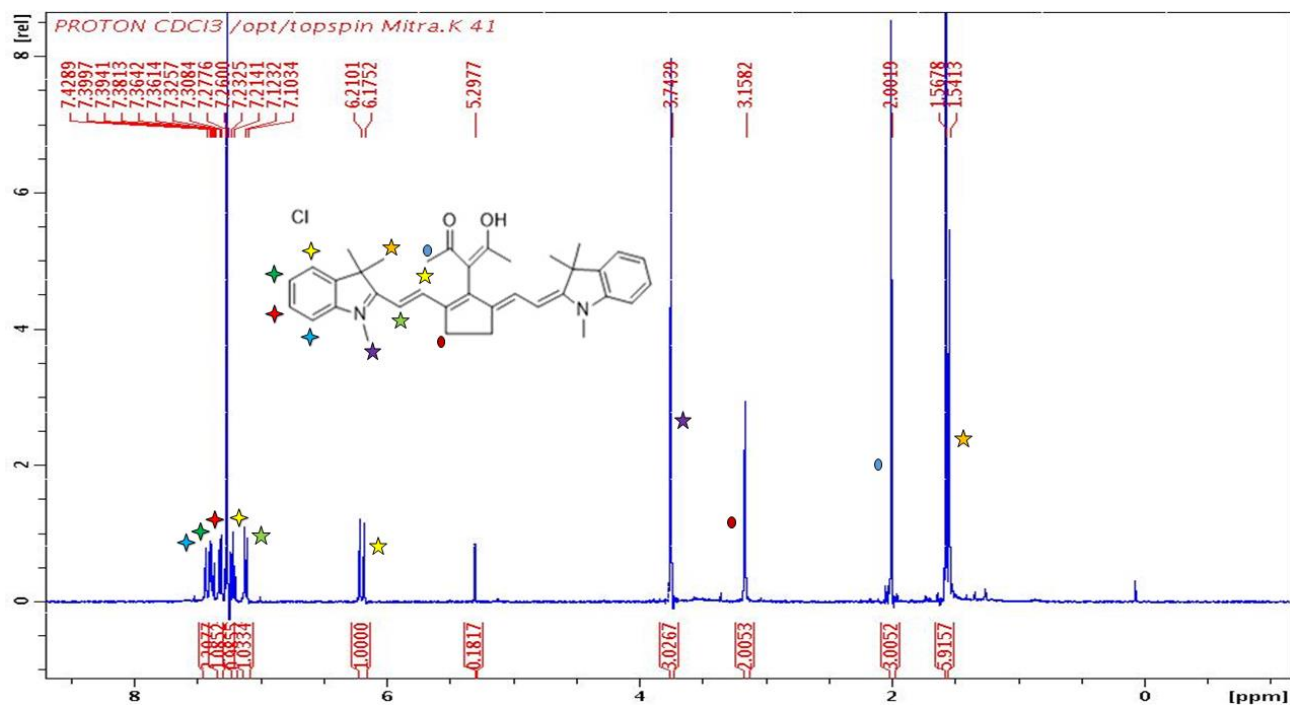


Figure S2. ^1H NMR spectra of the ligand IR797-acac recorded in CDCl_3 . Cationic structure is shown.

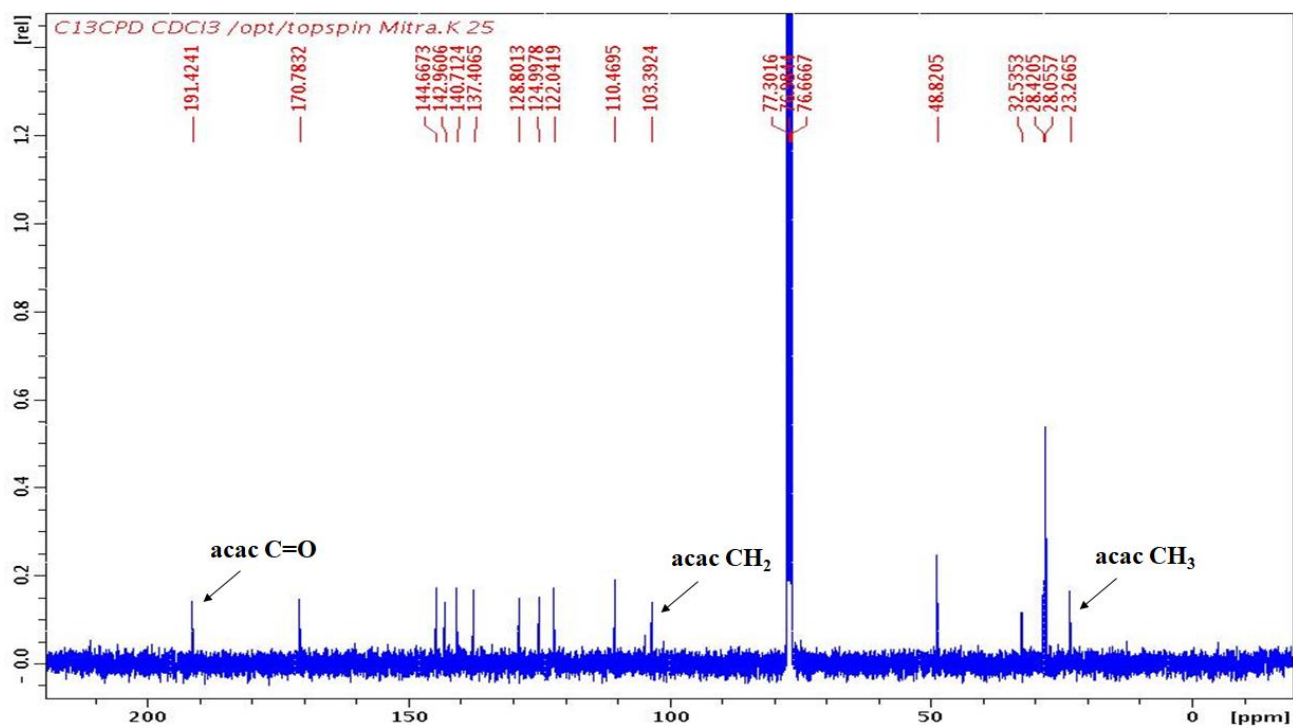


Figure S3. ^{13}C NMR spectra of the ligand IR797-acac recorded in CDCl_3 .

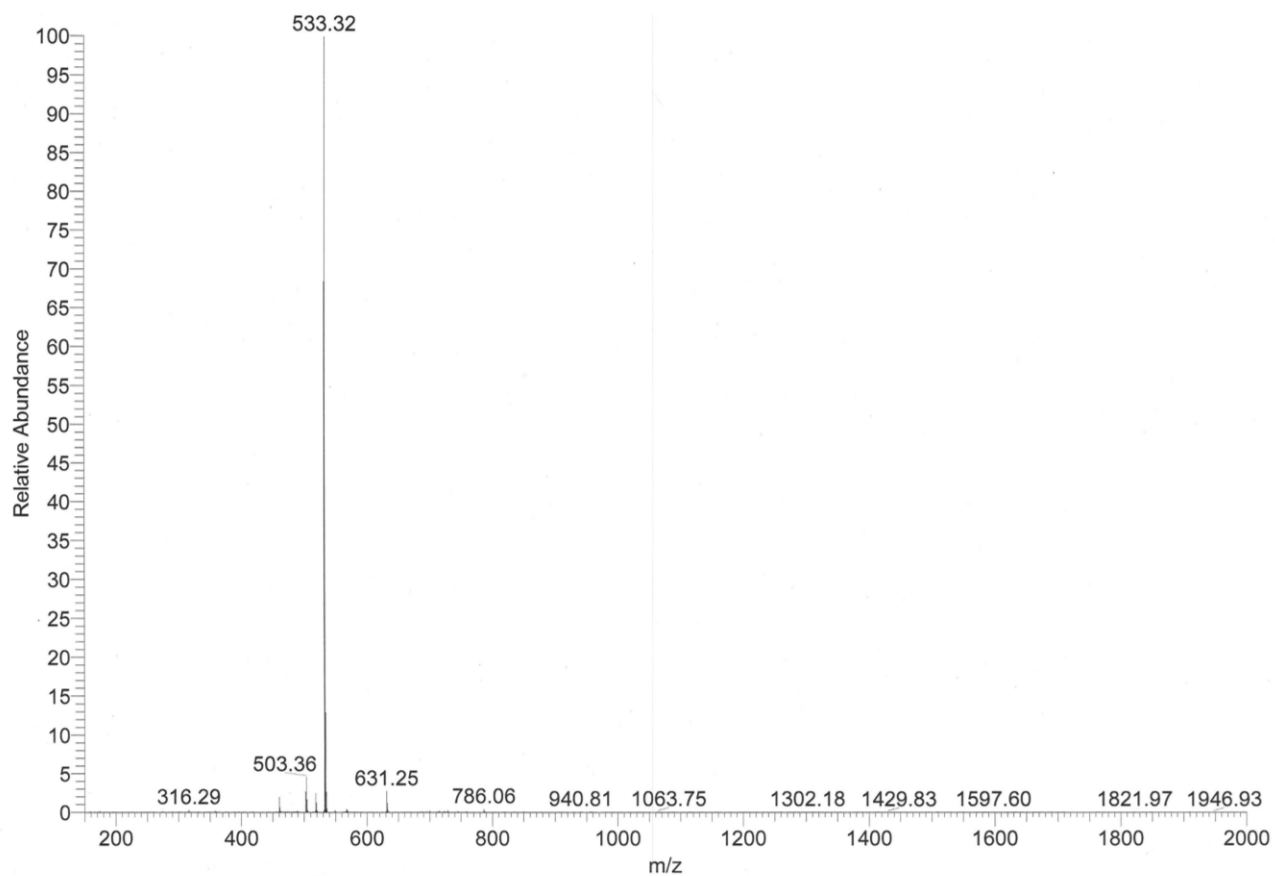


Figure S4. ESI-MS of ligand IR797-acac (Formula: $C_{36}H_{41}ClN_2O_2$, Molecular Weight: 569.19) in acetonitrile showing m/z peak at 533.32 for $[M-Cl]^+$ ions (100% abundance). Expected m/z was 533.33.

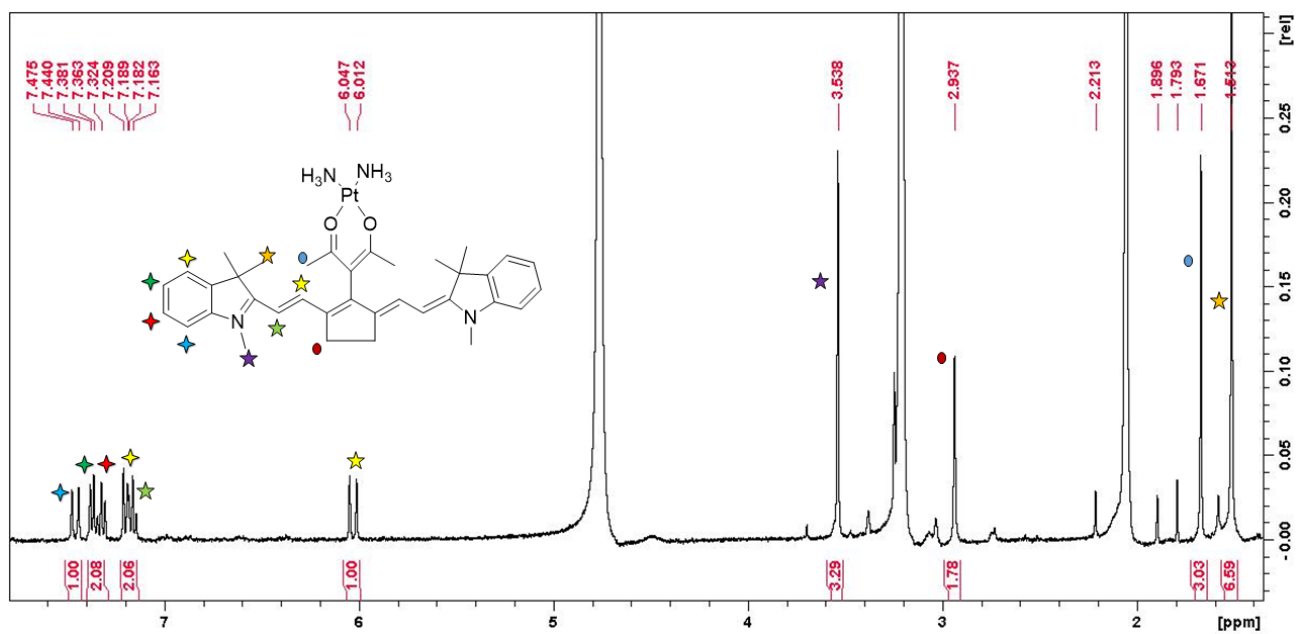


Figure S5. ^1H NMR spectra of complex **1** in methanol- d_4 . Cationic structure is shown.

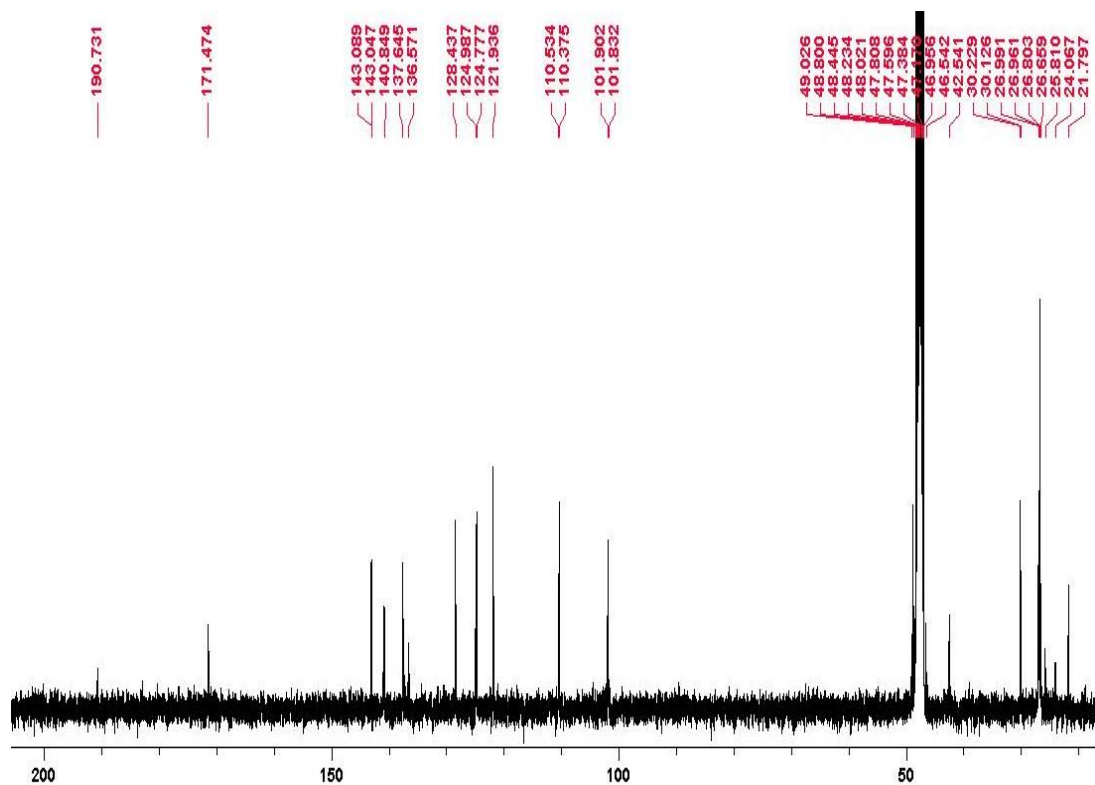


Figure S6. ^{13}C NMR spectra of complex **1** in methanol- d_4 .

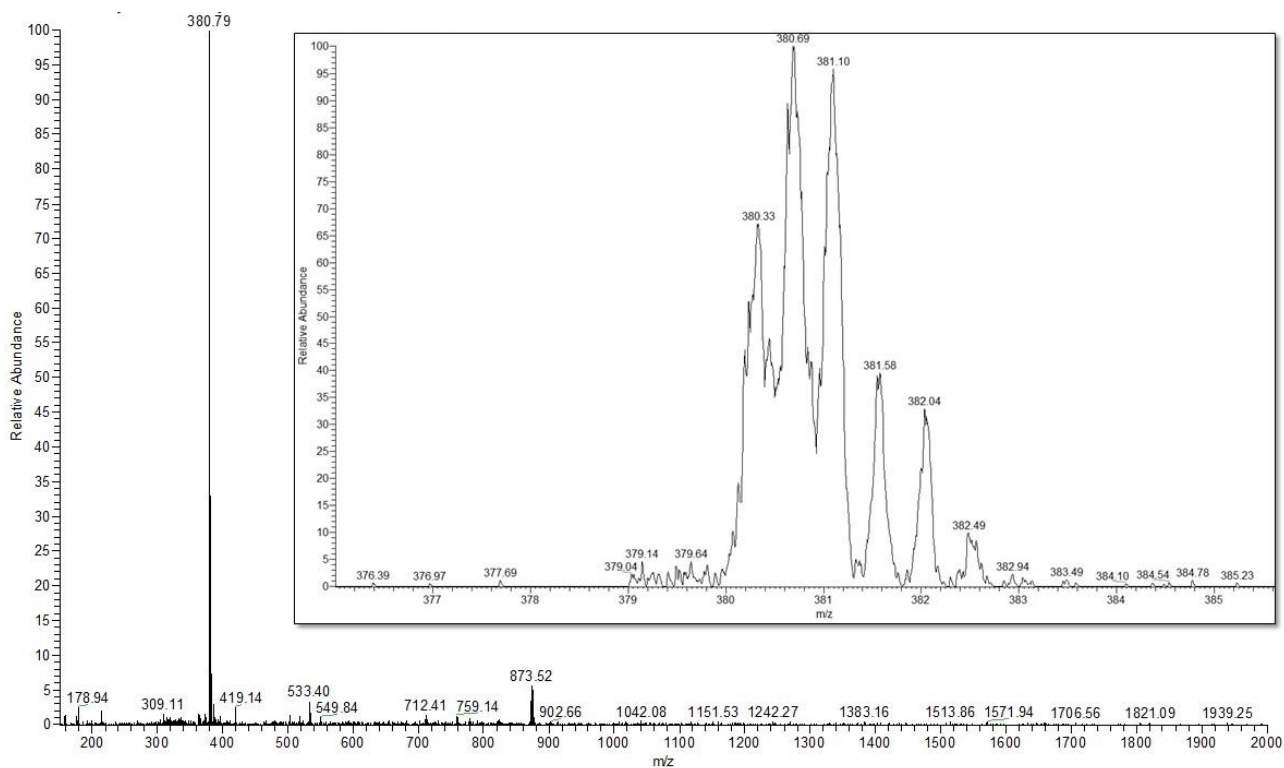


Figure S7. ESI-MS of complex **1** in acetonitrile showing the m/z peak at 380.69 for $[M-Cl-NO_3]^{2+}$ ions (100% abundance). Expected m/z for **1** (Formula: $C_{36}H_{46}ClN_5O_5Pt$, Molecular Weight: 859.33) was 380.60. The inset of the figure is the zoom MS scan showing the isotopic distribution of Pt and two units of positive charge in the fragment.

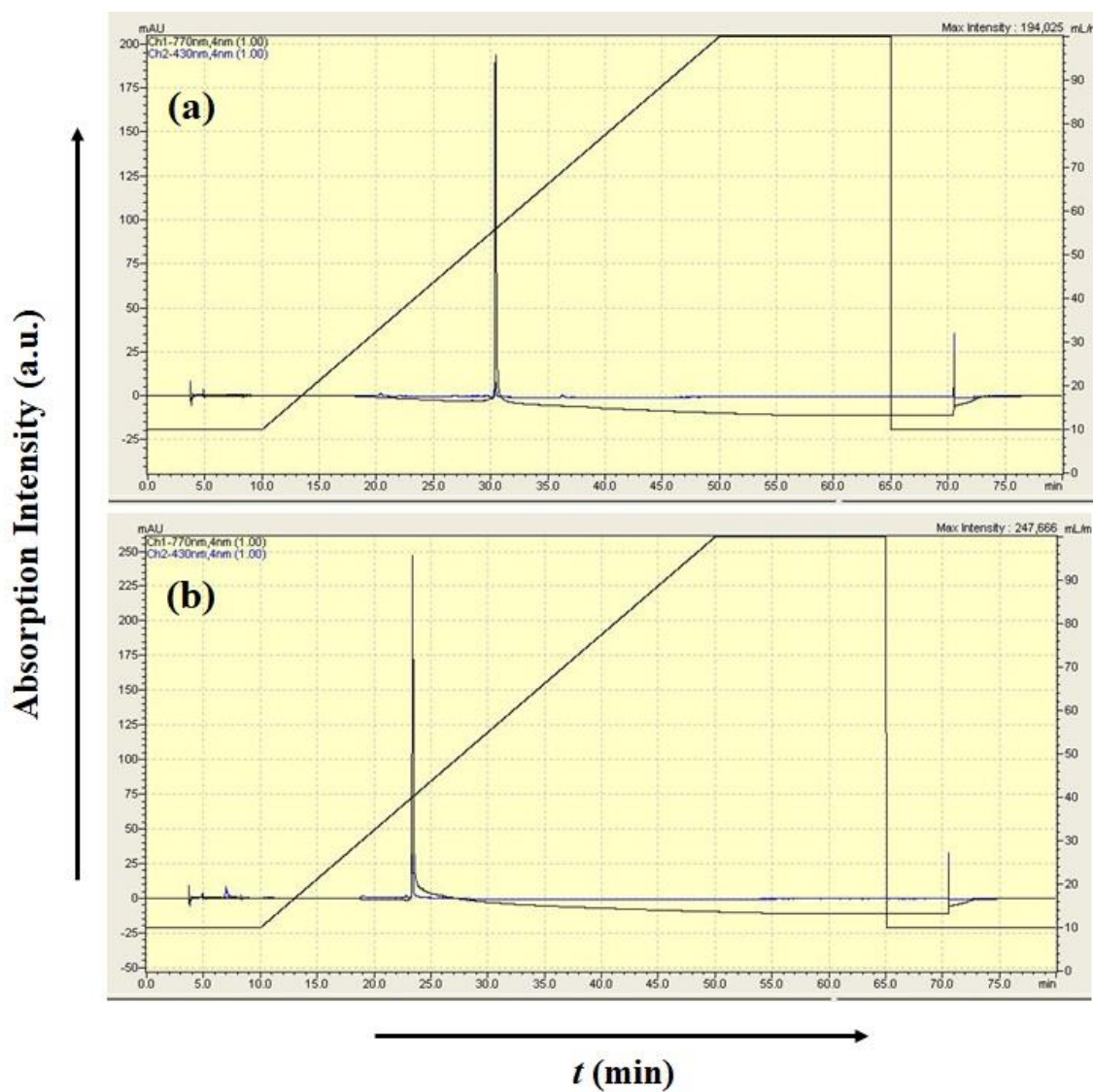


Figure S8. HPLC chromatograms of (a) IR797-acac and (b) complex **1** using 10-100% acetonitrile-water gradient. The ligand appeared at 30 min while complex **1** exhibited a peak at 24 min. The absorbance was monitored at two wavelengths of 430 nm and 770 nm.

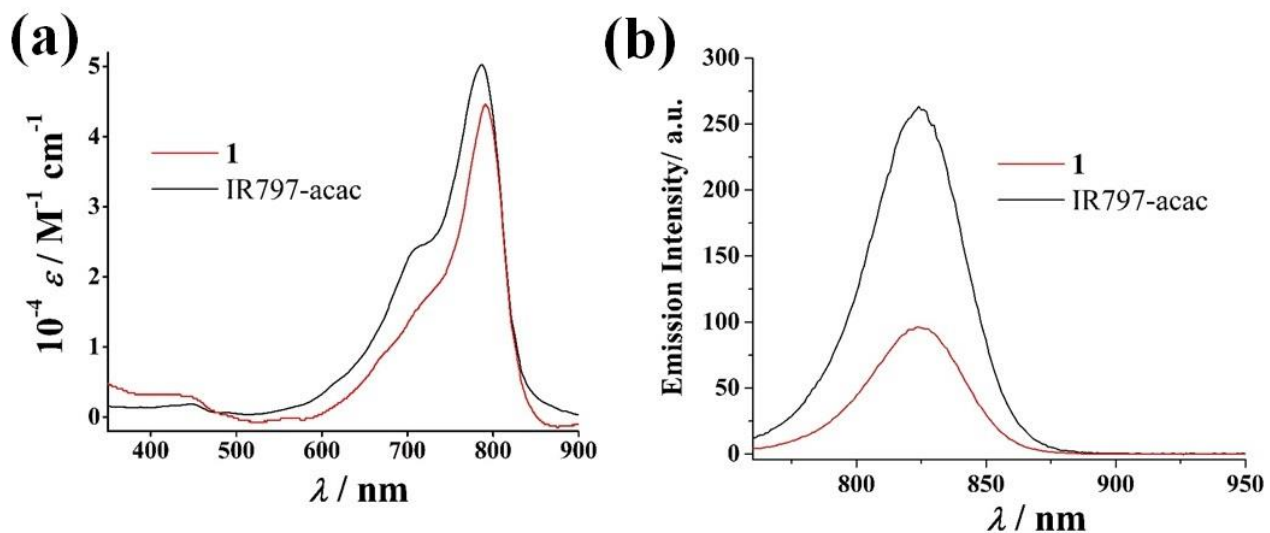


Figure S9 (a) Absorption spectra and (b) emission spectra of complex **1** and IR797-acac in 0.1% DMSO-PBS at pH 7.4.

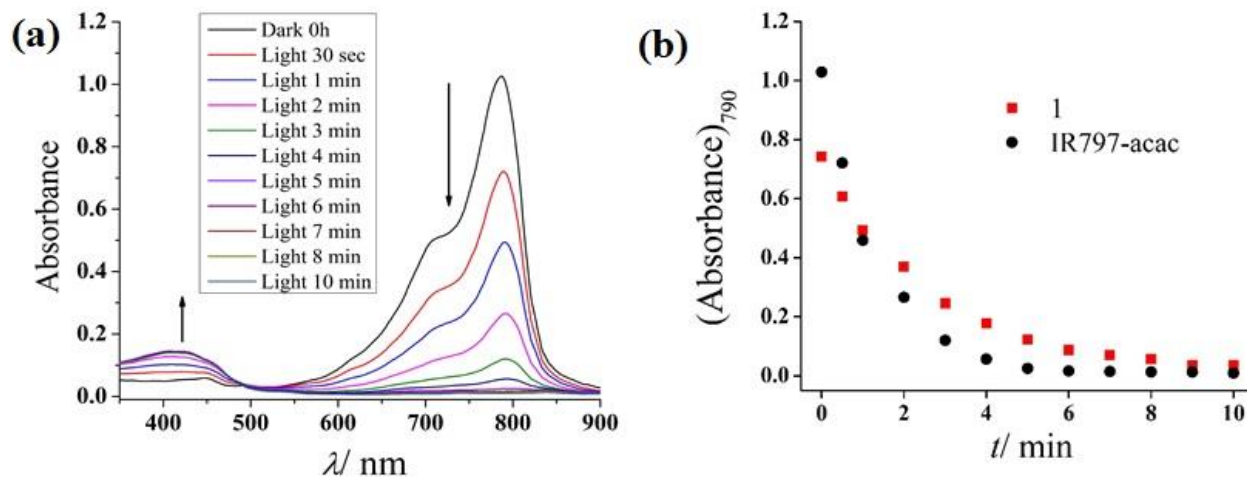


Figure S10. (a) Irradiation time dependent loss of absorption intensity at 790 nm of IR797-acac in 0.1 % DMSO-PBS (pH = 7.4). (b) Scatter plots of the same experiment showing absorbance at 790 nm vs time for **1** and IR797-acac.

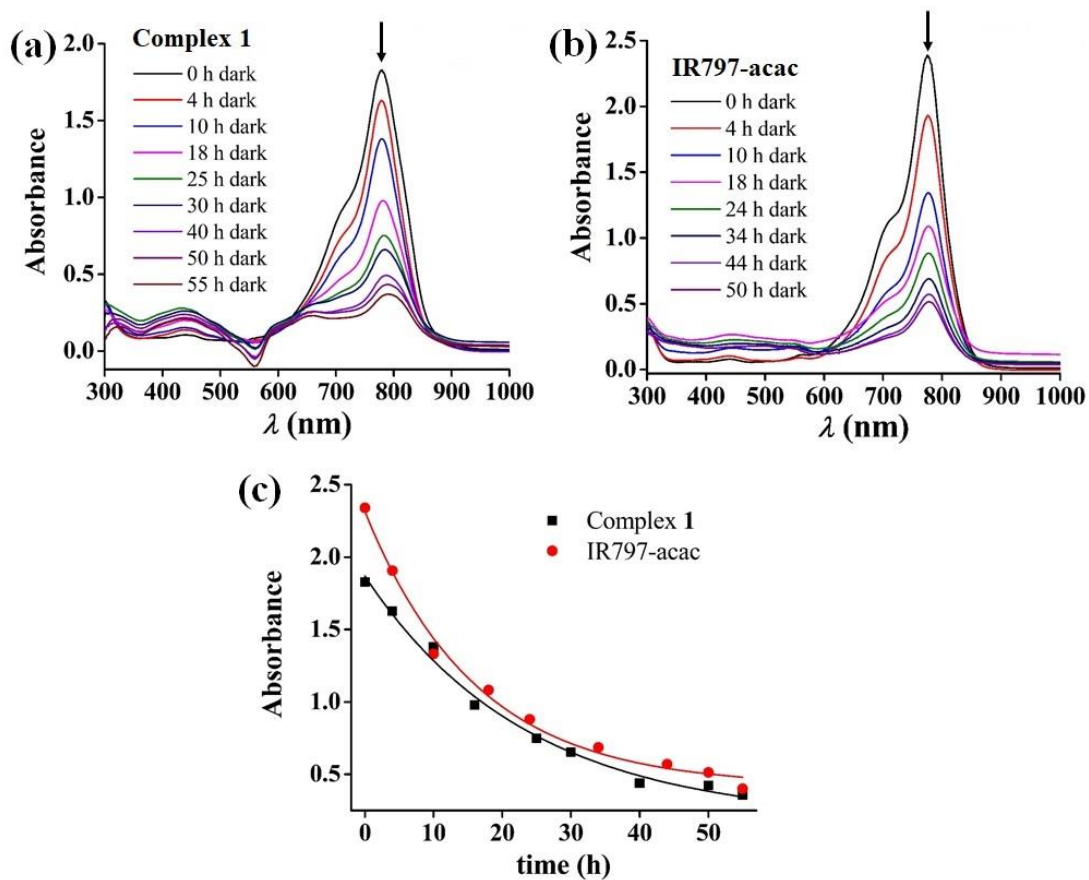


Figure S11. Stability studies in dark conditions of (a) complex **1** and (b) ligand IR797-acac in 0.5% DMSO-10% FBS-DMEM solutions demonstrated by monitoring absorption spectra at different time points as denoted in the graph. (c) Scatter plots of the same experiments showing absorbance at 790 nm vs. time and the corresponding exponential fit was performed to obtain the half-lives.

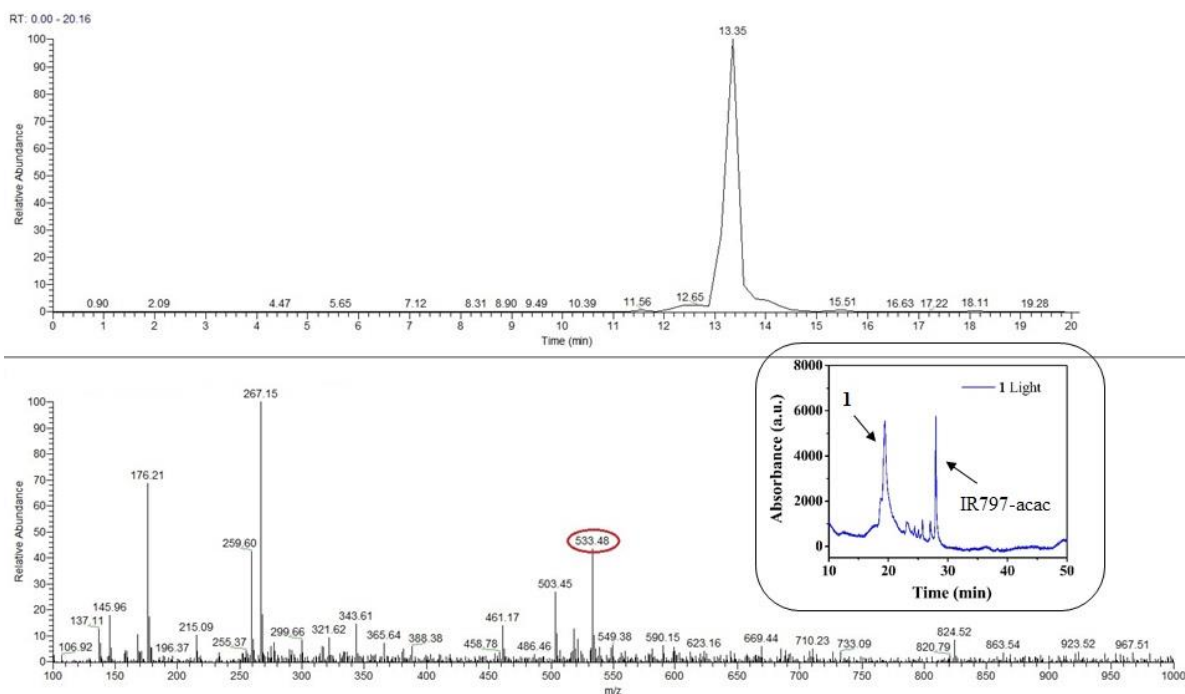


Figure S12. LC-MS chromatogram trace and the corresponding mass spectra showing release of the free ligand IR797-acac (m/z found = 533.5, expected for $[M-Cl]^+ = 533.3$) from the Pt(II) center photoexposed samples of photoexposed complex **1** (1 min, 720-740 nm). Inset shows HPLC chromatogram of the photoexposed solution of **1** (1 min, 720-740 nm) showing peak for ligand IR797-acac (at 29 min) along with undecomposed **1** (at 20 min) and other minor photoproducts. The major fractions appearing at 20 and 29 min was collected (monitored at 430 nm) and verified by mass spectroscopy and assigned as complex **1** and free IR797-acac.

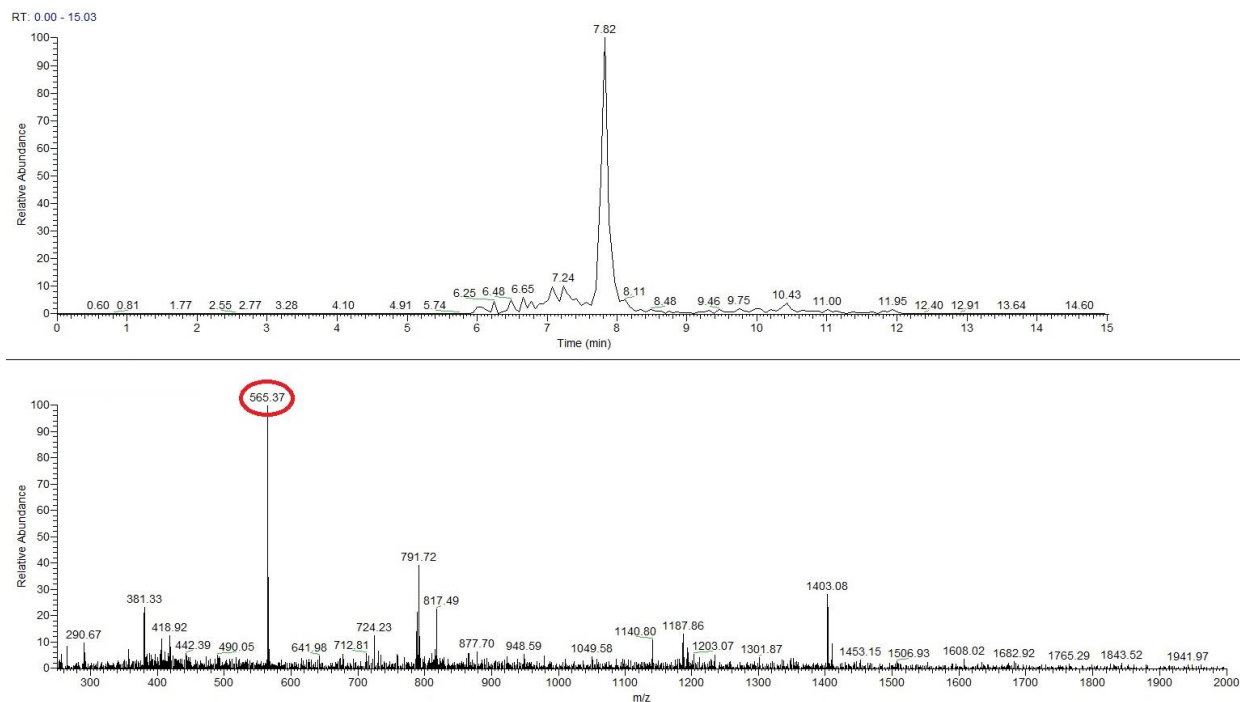


Figure S13. LC-MS chromatogram trace and the corresponding mass spectra showing formation of the 1,2-dioxetanes P1a/ P1b (m/z found = 565.4, expected for $[M+H]^+ = 565.6$) due to possible oxidation of the released ligand IR797-acac in photoexposed samples of complex **1** (15 min, 720-740 nm).

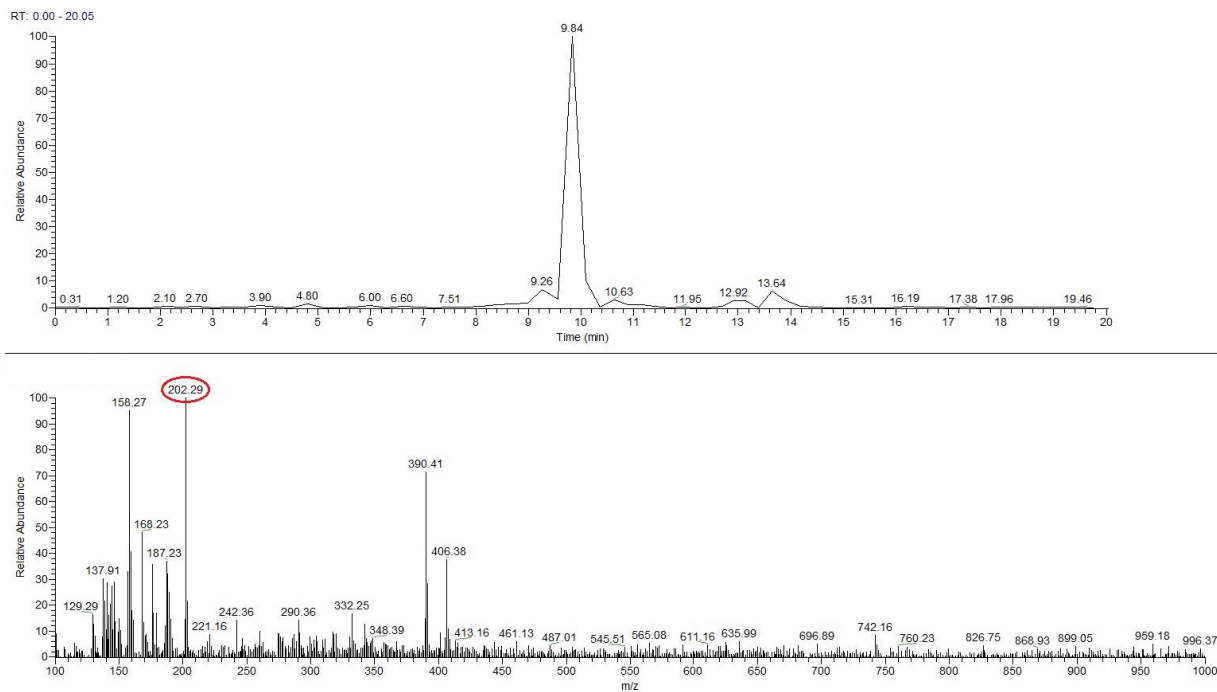


Figure S14. LC-MS chromatogram trace and the corresponding mass spectra showing formation of P2 (m/z found = 202.3, expected for $[M+H]^+ = 202.3$) in photoexposed samples of complex **1** (15 min, 720-740 nm, and incubated at 37°C for 1 h).

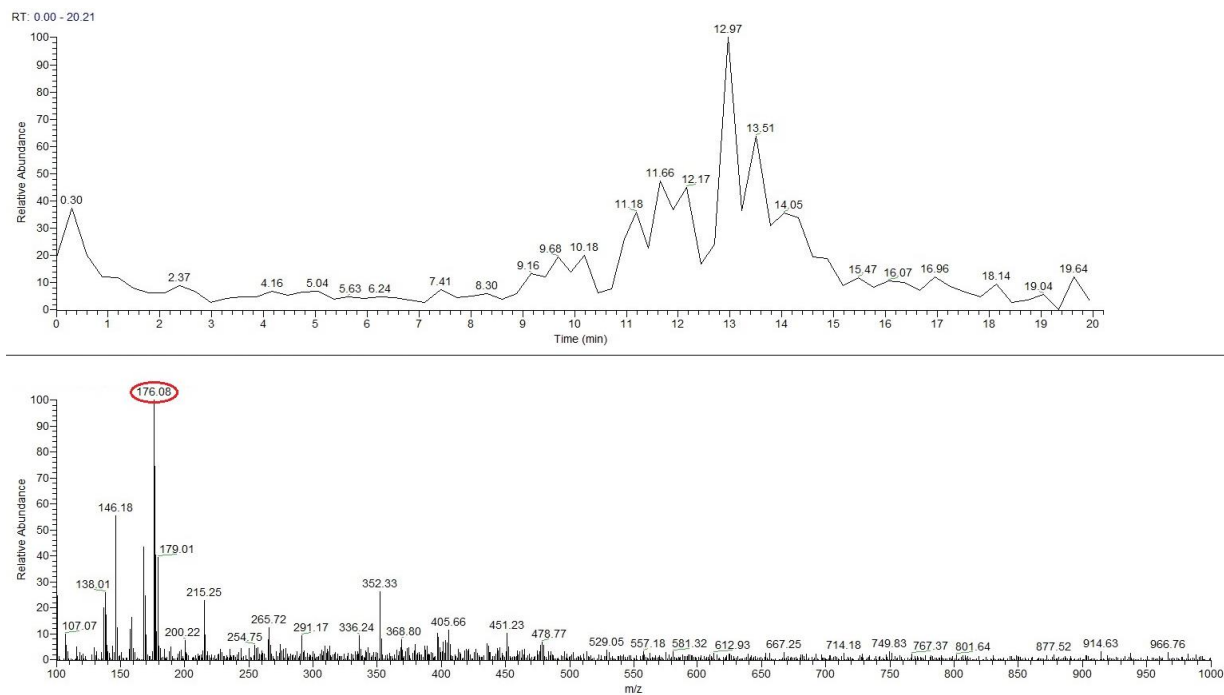


Figure S15. LC-MS chromatogram trace and the corresponding mass spectra showing formation of P3 (m/z found = 176.1, expected for $[M+H]^+ = 176.2$) in photoexposed samples of complex **1** (15 min, 720-740 nm, and incubated at 37°C for 1 h).

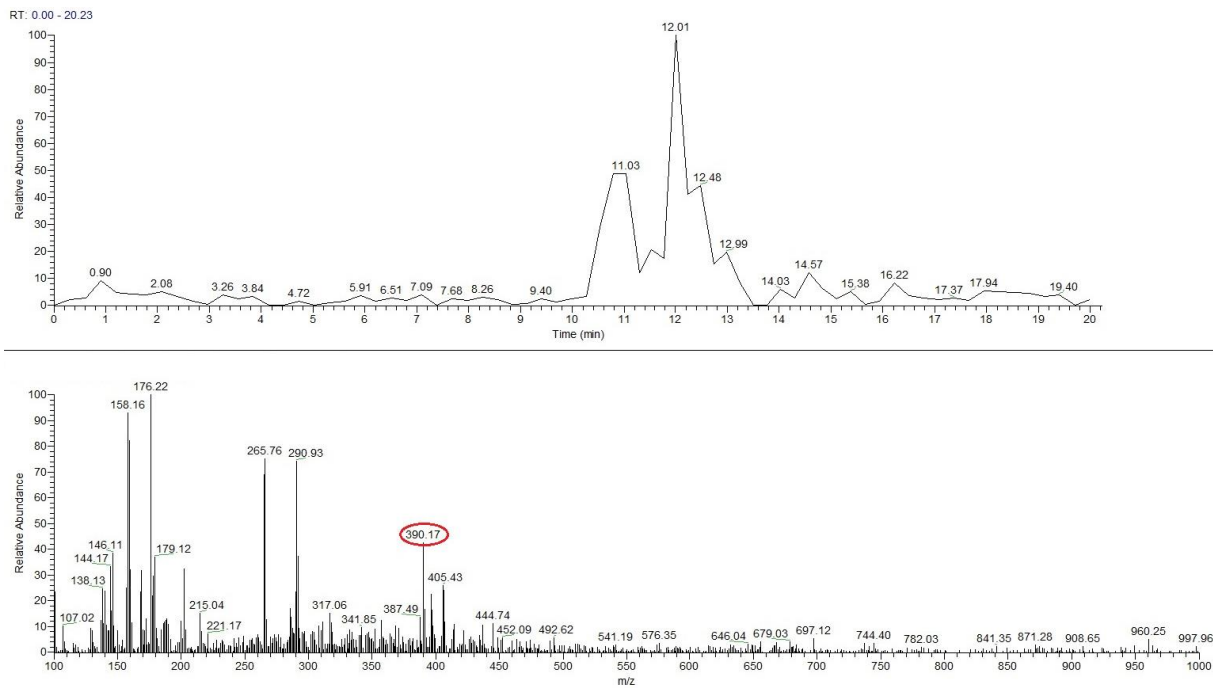


Figure S16. LC-MS chromatogram trace and the corresponding mass spectra showing formation of P4 (m/z found = 390.2, expected for $[M-C1]^+ = 390.0$) in photoexposed samples of complex **1** (15 min, 720-740 nm, and incubated at 37°C for 1 h).

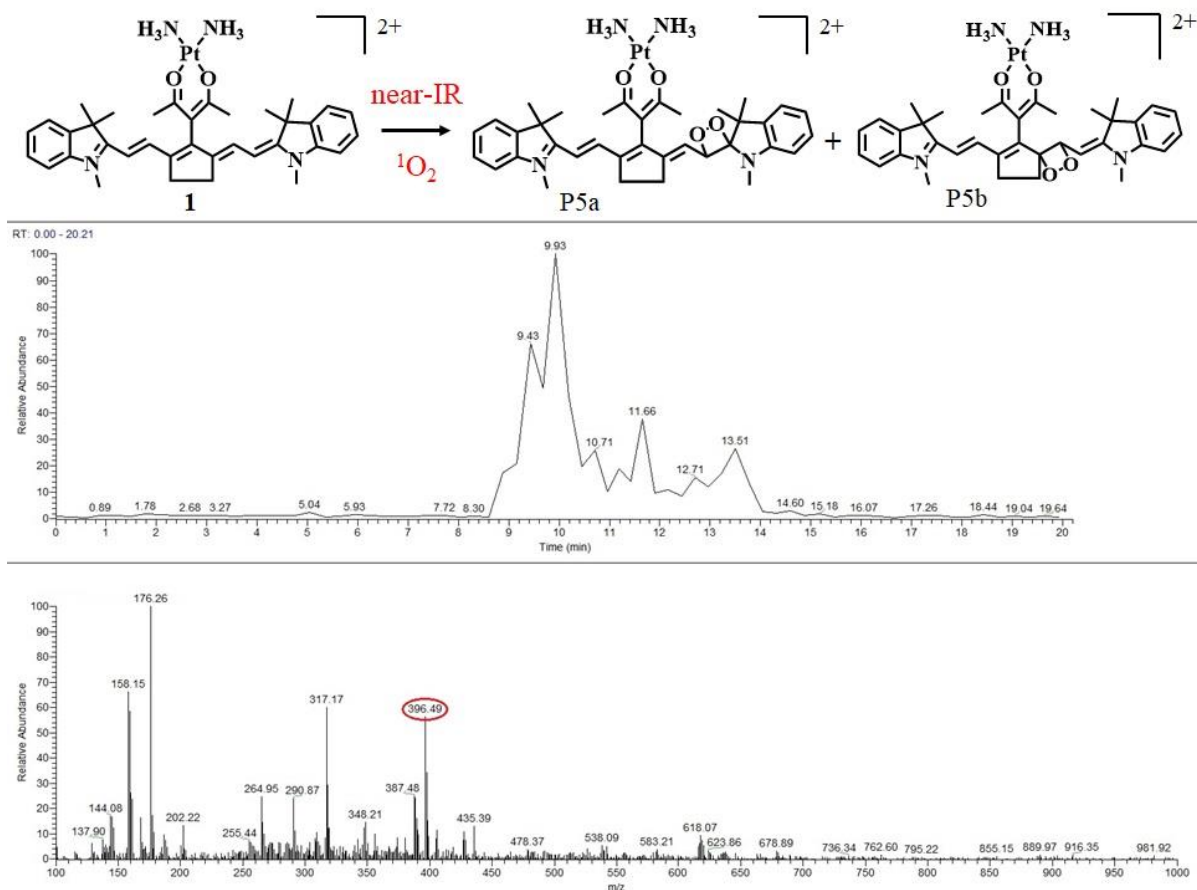


Figure S17. LC-MS chromatogram trace and the corresponding mass spectra showing formation of P5a/ P5b (m/z found = 396.5, expected for $[M]^{2+} = 396.5$) in photoexposed samples of complex **1** (15 min, 720-740 nm). Zoom MS scan showed the isotopic distribution pattern for Pt with a spacing correlating to +2 charge.

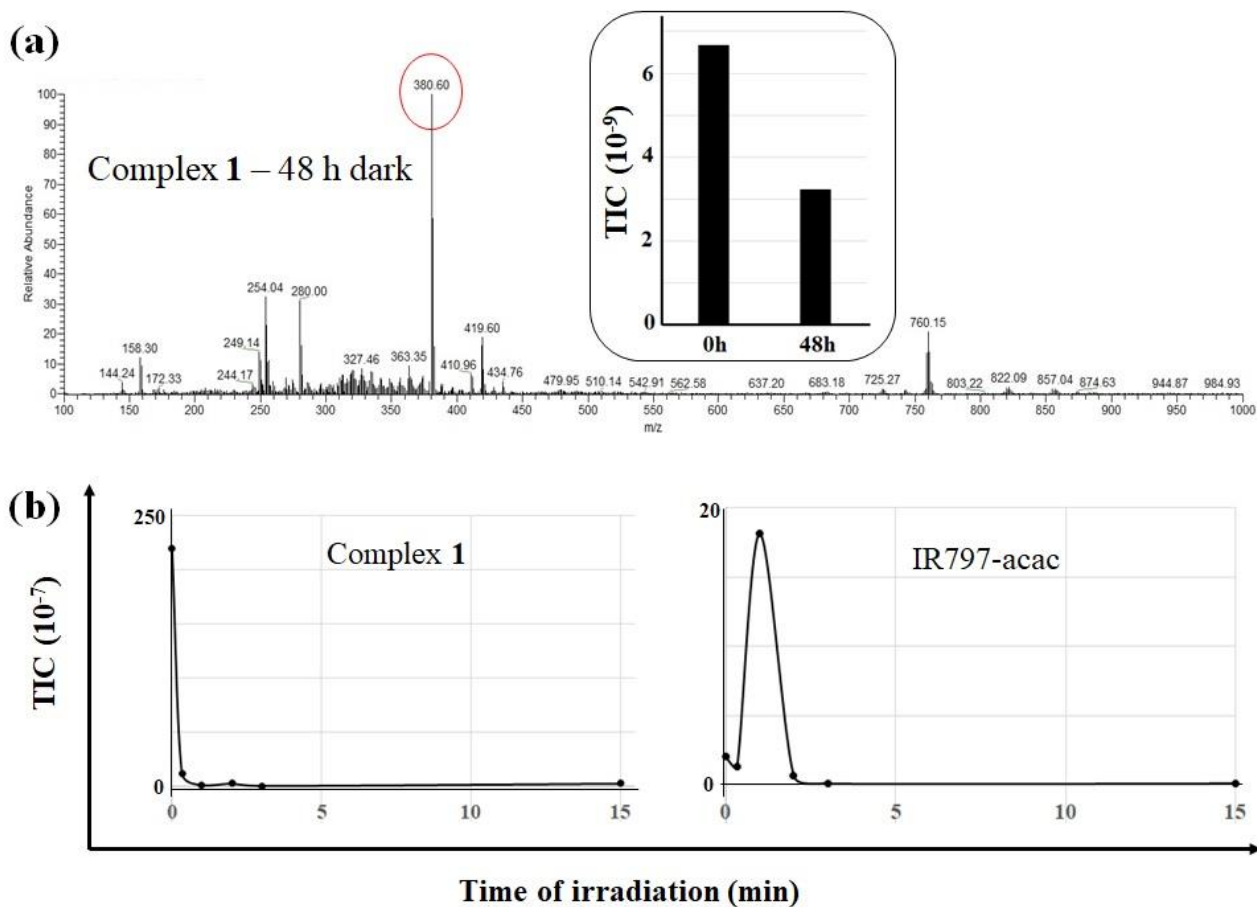


Figure S18. (a) Stability of complex **1** in absence of light demonstrated by LC-MS experiments of a sample kept in the dark for 48 h showing the highest abundant peak at m/z of 380.6 which is assignable to the $[M-NO_3-Cl]^{2+}$ ion of **1**. Inset of figure shows total ion count (TIC) at 0 h and 48 h (dark) as obtained from LC-MS experiments. (b) LC-MS experiments showing loss of ion counts of complex **1** and appearance and consequent disappearance of ligand IR797-acac as plotted against irradiation time (0, 30 sec, 1 min, 2 min, 3 min, 15 min) of photoexposure of complex **1** (720-740 nm).

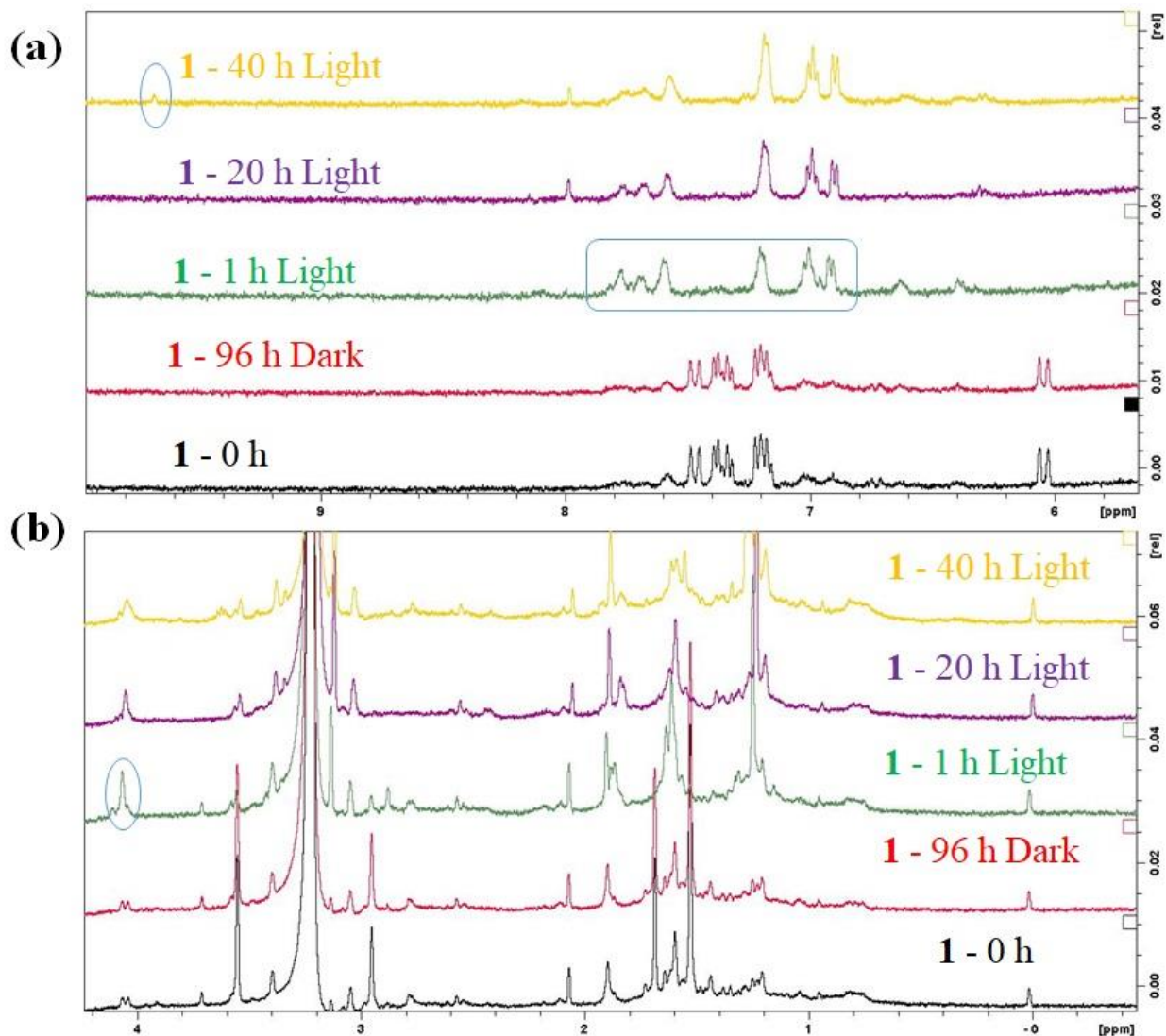


Figure S19. ^1H NMR of complex **1** recorded in methanol- d_4 showing expansion in the region (a) 6-10 ppm and (b) 0-4.5 ppm demonstrating formation of different photoproducts on irradiation. Irradiation was performed in the NMR tubes and data (512 scans) was recorded at time intervals (0 h, 1 h, 20 h and 40 h, 720-740 nm, $3.5 \pm 1.5 \text{ mW}\cdot\text{cm}^{-2}$) as shown in the graph. The disappearance of peaks corresponding to the complex in the region 7.1 – 7.5 ppm indicated photodecomposition. The new signals (shown with blue circles and square) appearing at 9.8 (for aldehyde proton) and in the 6.8-7.8 ppm (aromatic protons), 4.2 ppm (methylene protons) were assignable to the products P2 and P3 (see Fig. S20). Other products could not be assigned due to overlap and broadening of signals. The complex was stable in dark up to 96 h as evident from no considerable change in NMR spectra.

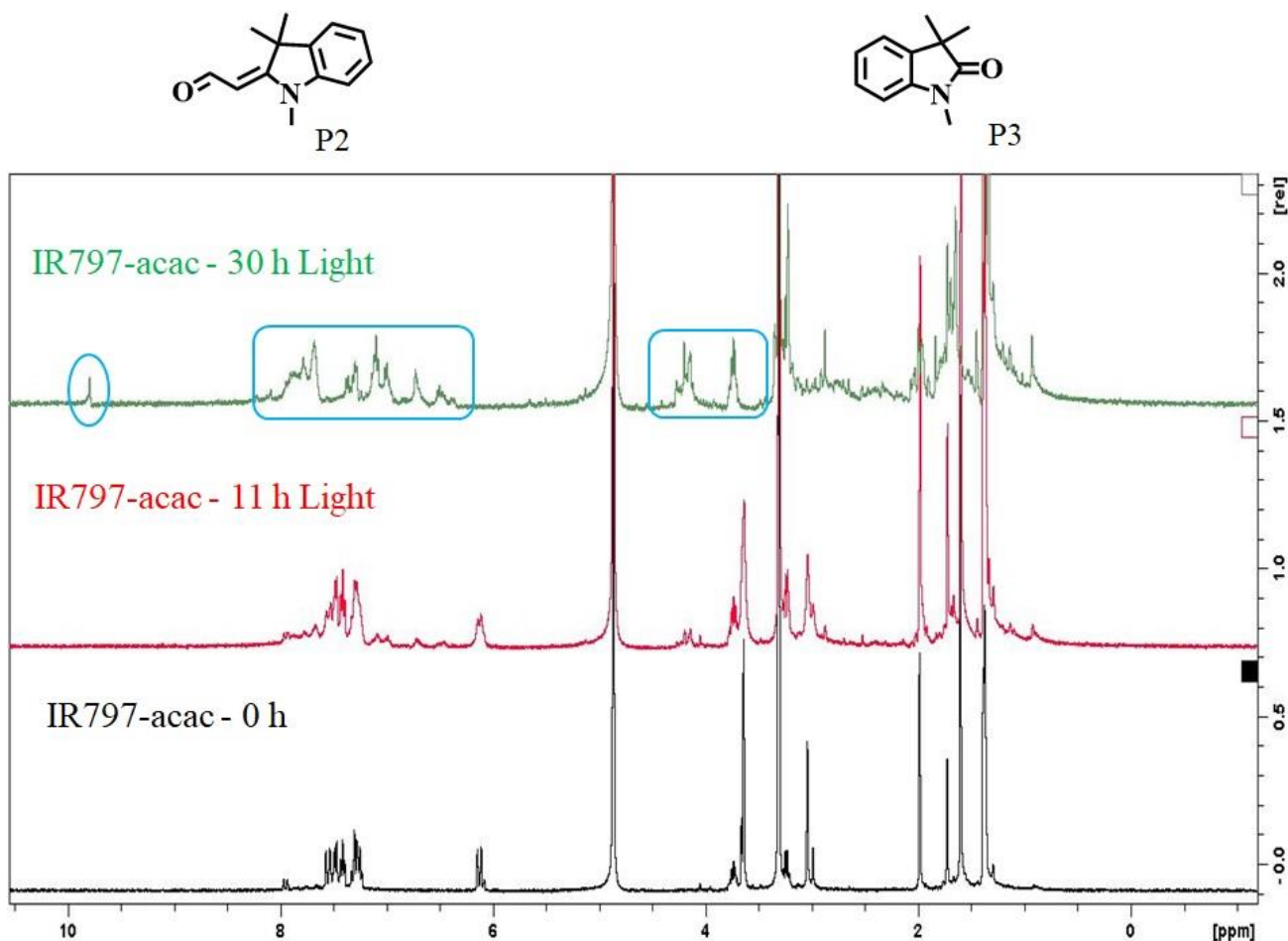


Figure S20. (a) ^1H NMR of IR797-acac recorded in methanol- d_4 showing formation of photoproducts on prolonged photoirradiation performed in the NMR tube (recorded at 0 h, 11 h and 30 h intervals, 720-740 nm, $3.5 \pm 1.5 \text{ mW}\cdot\text{cm}^{-2}$). On short irradiation times of 1 to 5 h, there were no changes in the NMR spectra which indicates sluggish dissociation rates in deuterated solvents. The signals at 6.1 ppm and in the region 7.2-7.6 ppm disappeared indicating degradation of IR797-acac. The new signals (shown with blue circle and squares) appearing at 9.8 (for aldehyde proton) and in the 6.5-7.9 ppm (aromatic benzene protons), 3.7-4.2 ppm (methylene protons) were assignable to the products P2 and P3. Other products could not be assigned due to overlap and broadening of signals.

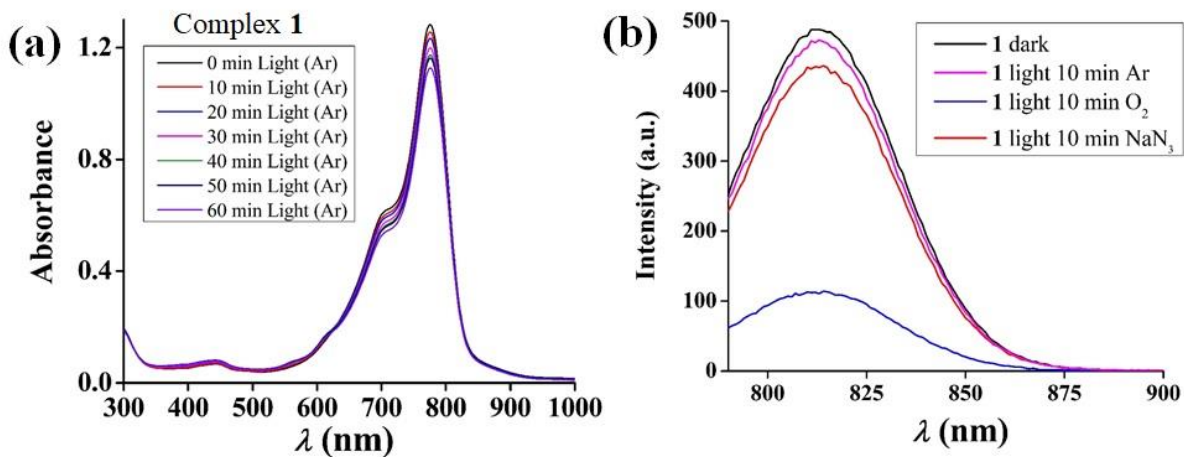


Figure S21. (a) Changes in absorption spectra of complex **1** in 1% DMSO-PBS solution on irradiation (Light, 720-740 nm, 3.5 ± 1.5 mW. cm^{-2}) under inert atmosphere for intervals as indicated in the graph. (b) Emission intensity of complex **1** ($3 \mu\text{M}$ in 1% DMSO-PBS, excitation at 760 nm) recorded in samples either kept in dark or photoexposed (light, 10 min, 720-740 nm) in various conditions: in argon (Ar); or in air (O_2) in presence of sodium azide (NaN_3 , $150 \mu\text{M}$). Sodium azide can act as singlet oxygen scavenger and was used to emphasize the role of singlet oxygen for photooxidation.

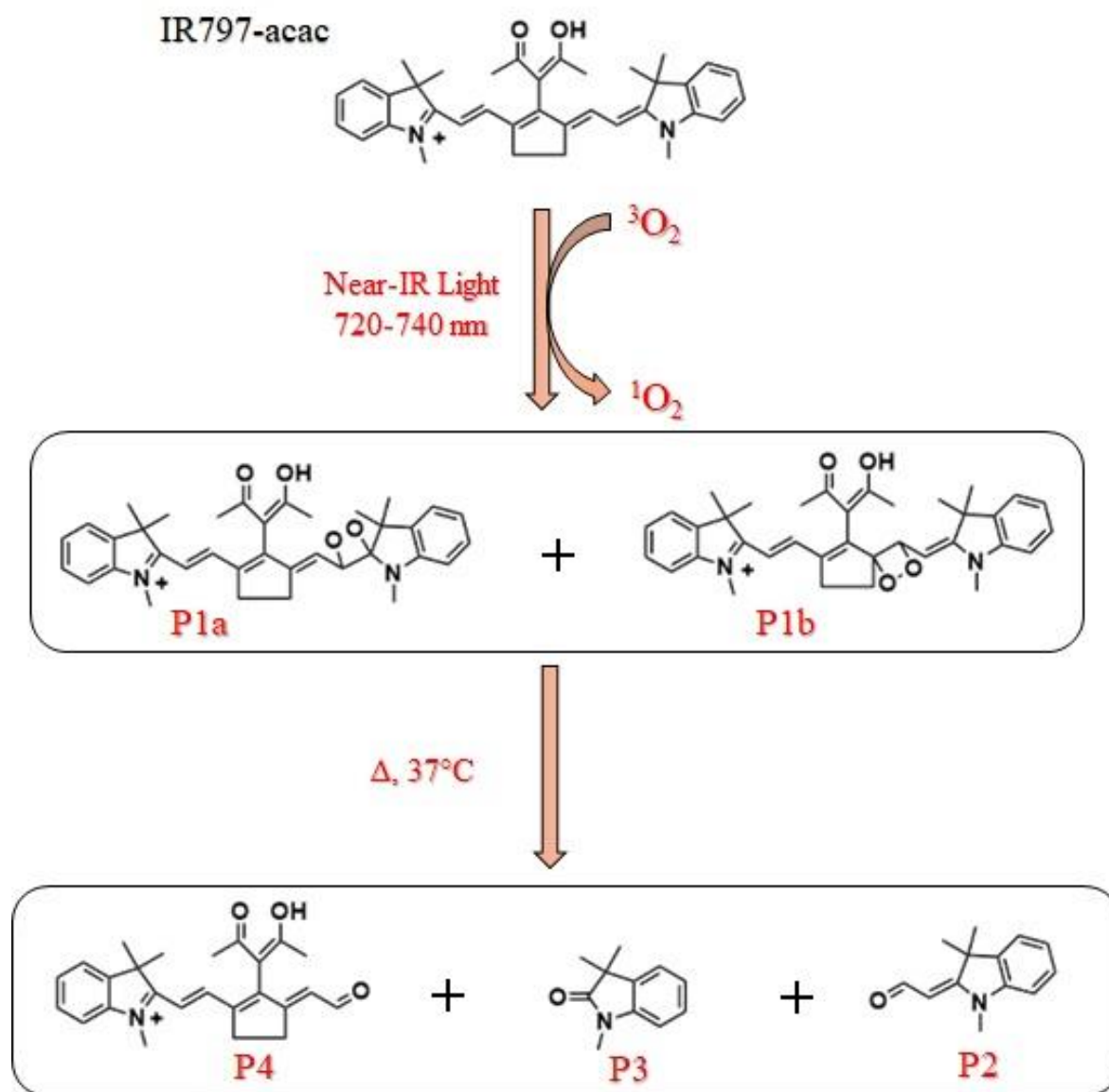


Figure S22. Mechanism of photodegradation of IR797-acac in 0.1% DMSO-PBS solutions, pH = 7.4. The peroxides P1a and P1b degrade thermally when warmed to 37 °C to form products P2-P4.

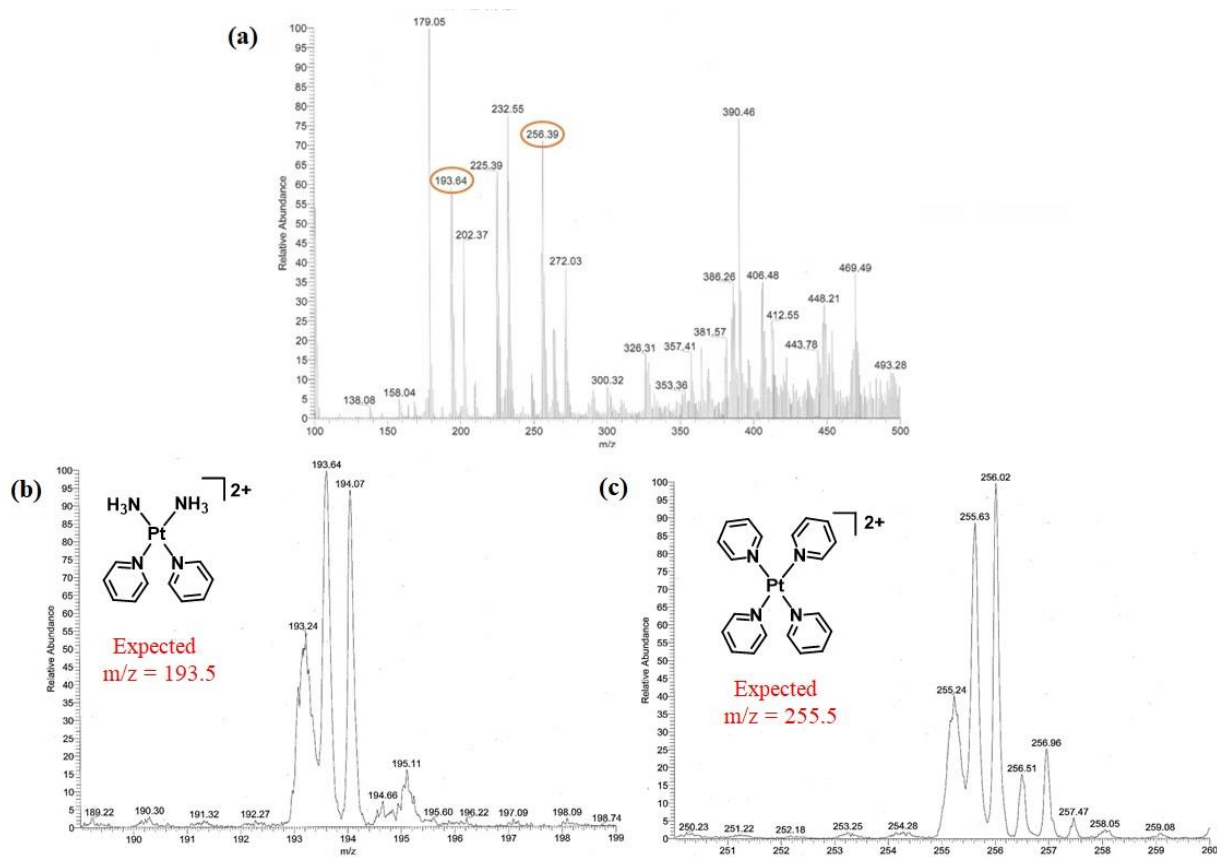


Figure S23. (a) ESI-MS spectra of samples containing complex **1** (20 μM in 0.1% DMSO-PBS) and pyridine (10 μl) irradiated with near-IR light (1 min, 720-740 nm) showing presence of peak assignable to pyridine substituted platinum(II) complexes as shown in figure. (b, c) ESI zoom scans were performed to show the +2 charge and Pt isotopic distribution of the specific masses of interest. The colour of the solution turned red from green on light exposure. Samples of complex **1** and pyridine kept in dark for 24 h showed minor adduct formation. Samples of complex **1** irradiated without pyridine or IR797-acac irradiated with pyridine did not show the presence of these m/z peaks further confirming the possibility that these peaks are from Pt-pyridine adducts.

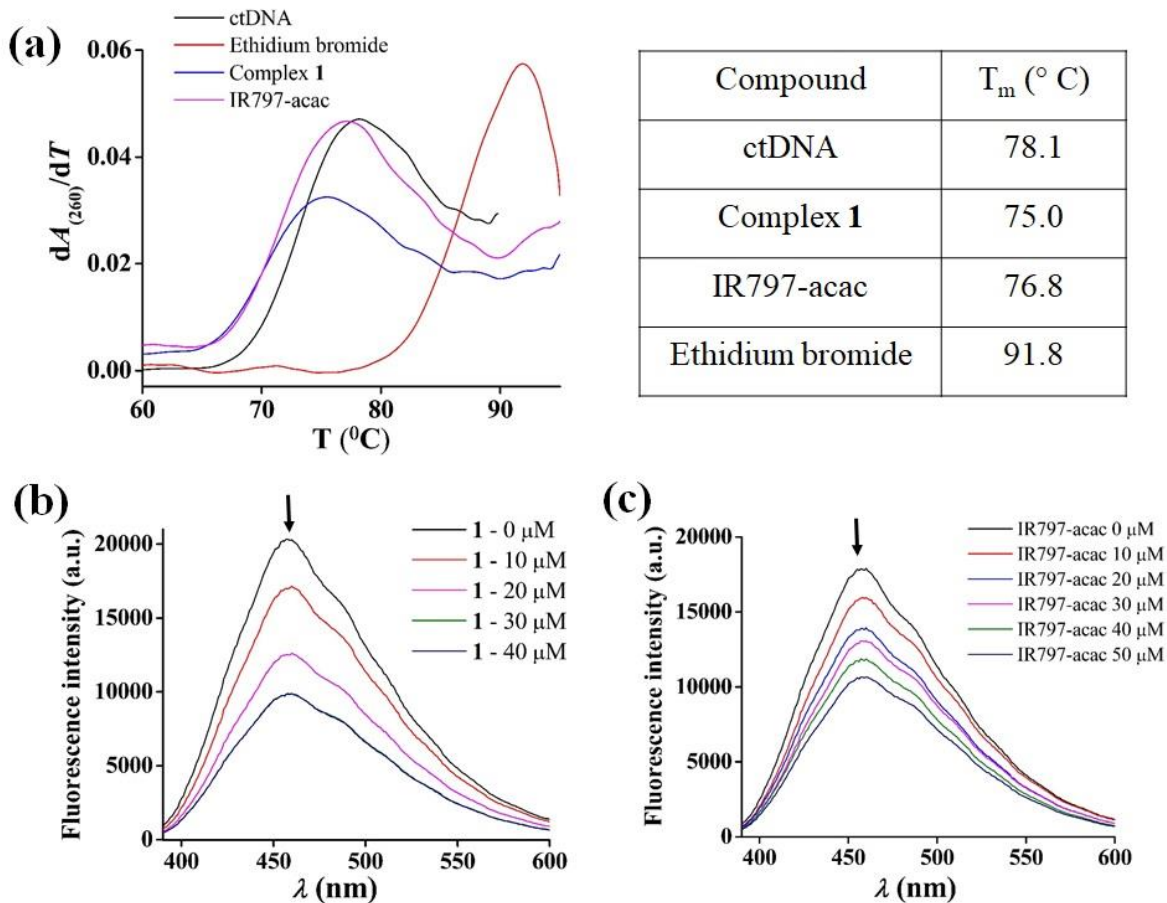


Figure S24. (a) DNA melting curves (derivative plots) of ctDNA (200 μM) alone or treated with complex **1**, IR797-acac or ethidium bromide (20 μM in 0.5% DMSO-PBS). The adjacent table shows the melting temperature (T_m) for the compounds. Complex **1** and IR797-acac showed small negative ΔT_m values of 1-3 $^\circ\text{C}$ indicating destabilizing interactions via minor groove binding. EB showed a huge positive ΔT_m values of 14 $^\circ\text{C}$ which is a result of intercalation to ctDNA. (b) and (c) Hoechst dye displacement assay using Hoechst 33342 dye which is known to interact with ctDNA via minor groove binding. The decrease in emission intensity on increasing concentration of complex **1** (b) and IR797-acac (c) evidenced the ability of the compounds to displace Hoechst dye and bind to DNA via the minor grooves. Excitation wavelength = 360 nm.

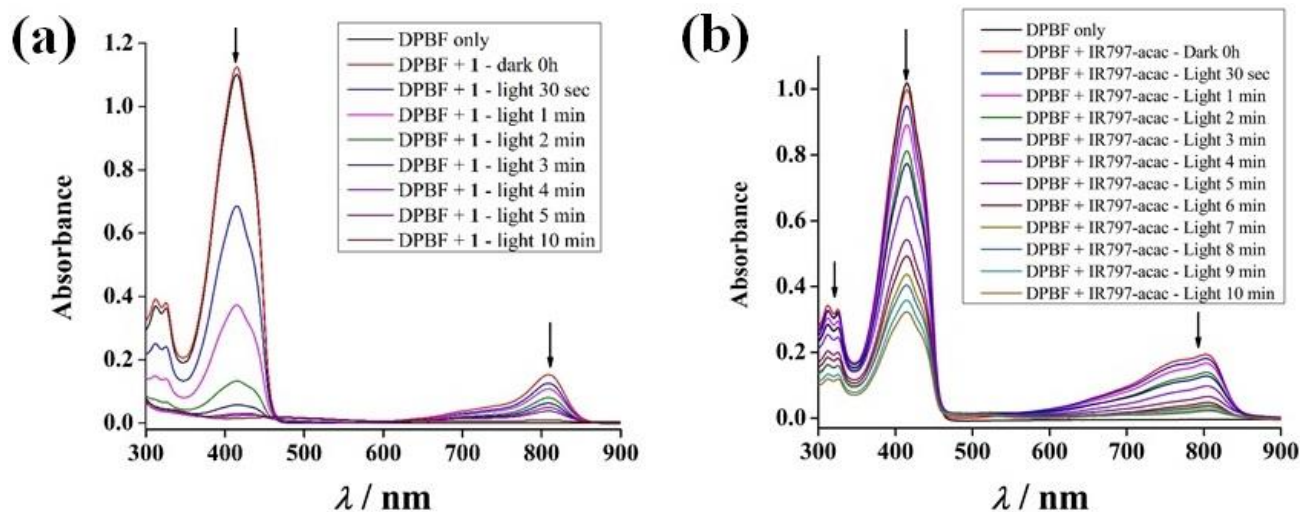


Figure S25. Absorption spectral traces of solutions containing DPBF and either (a) complex **1** or (b) IR797-acac ($3 \mu\text{M}$ in 0.1% DMSO-PBS) recorded at various time points after irradiation in near-IR light as depicted in the graph. The decrease in absorbance at 415 nm is a measure of generation of singlet oxygen in the solution. The absorbance at 790 nm also decreases because of the photobleaching of the compounds in near-IR light.

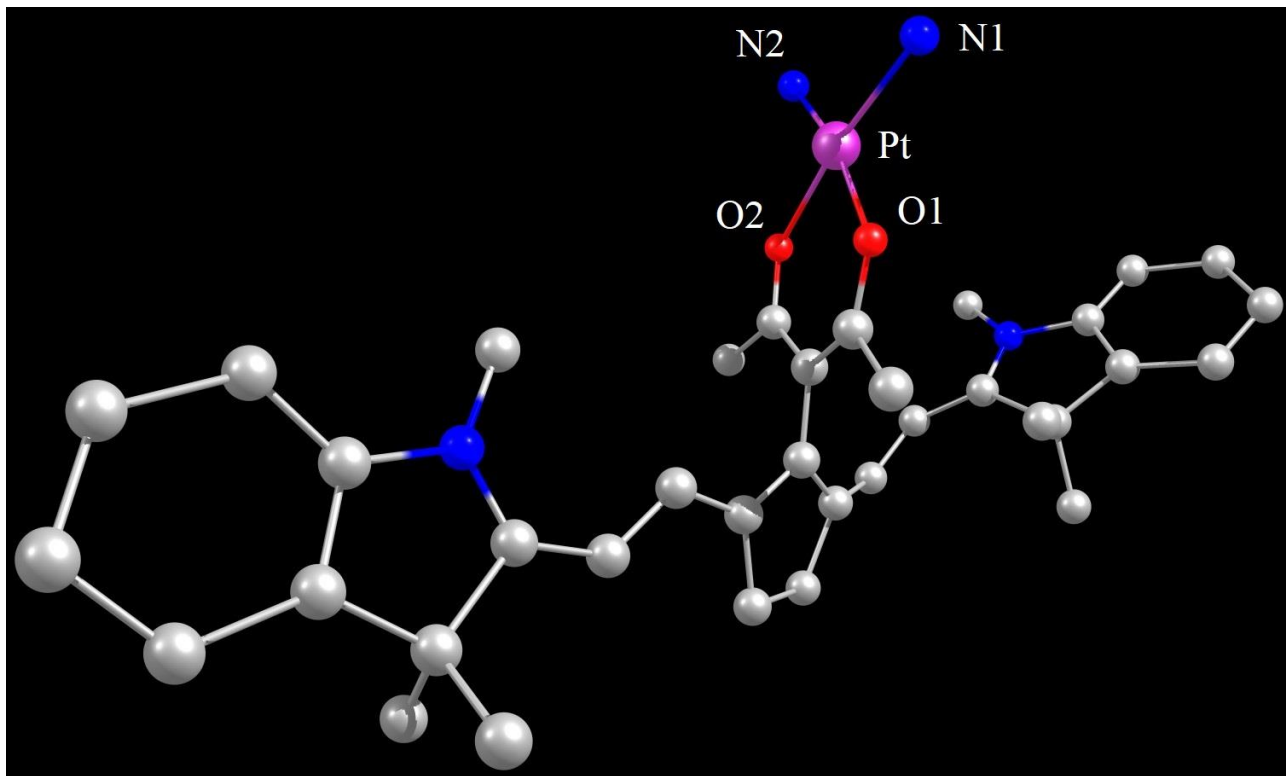


Figure S26. Optimized geometry of the triplet excited state of **1** using DFT calculations (B3LYP/LANL2DZ (for Pt) and 6-31+G (for rest of the atoms)). Colour codes: magenta, Pt; red, O; blue, N; gray, C. Hydrogens are omitted for clarity.

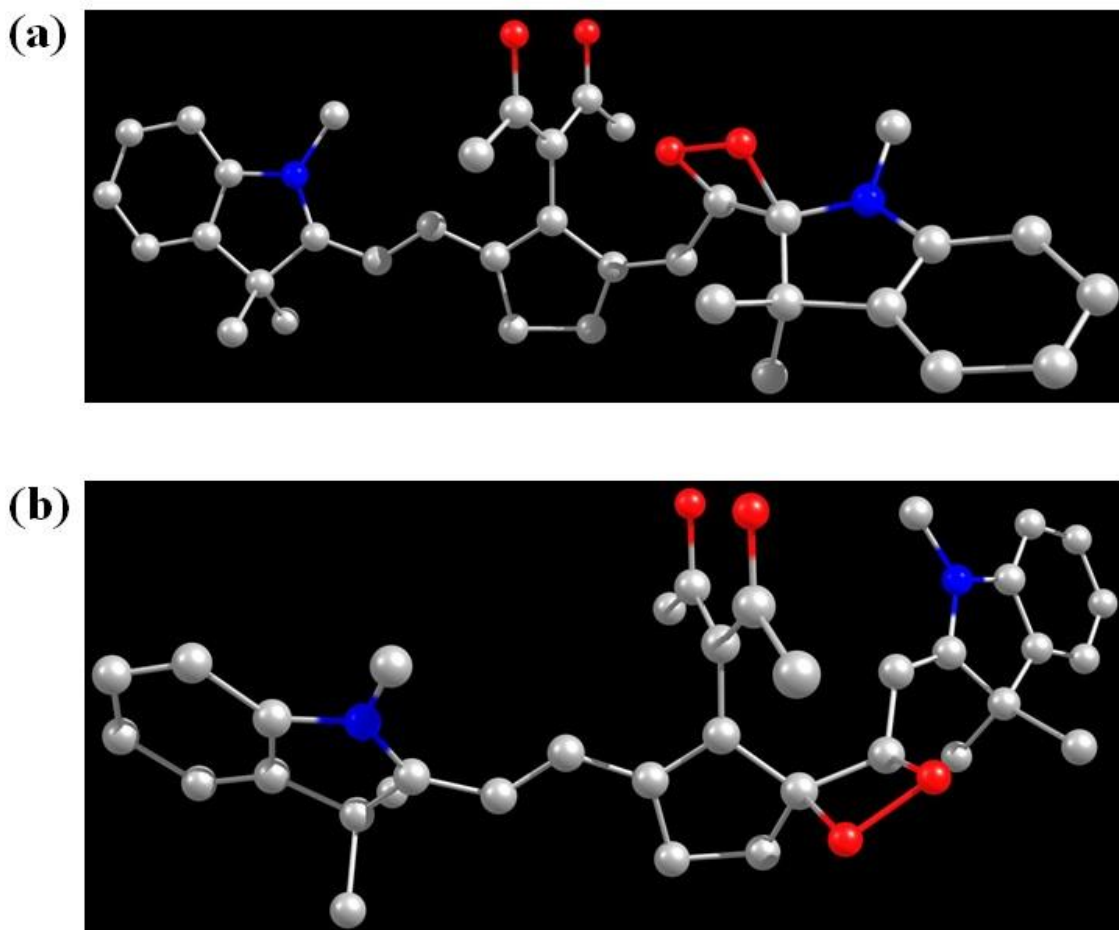


Figure S27. Geometry of optimized structures of (a) P1a and (b) P1b, the 1,2-dioxetanes formed due to photooxidation of ligand IR797-acac by DFT calculations using B3LYP/ 6-31+G functionals. Colour codes: red, O; blue, N; gray, C. Hydrogens are omitted for clarity.

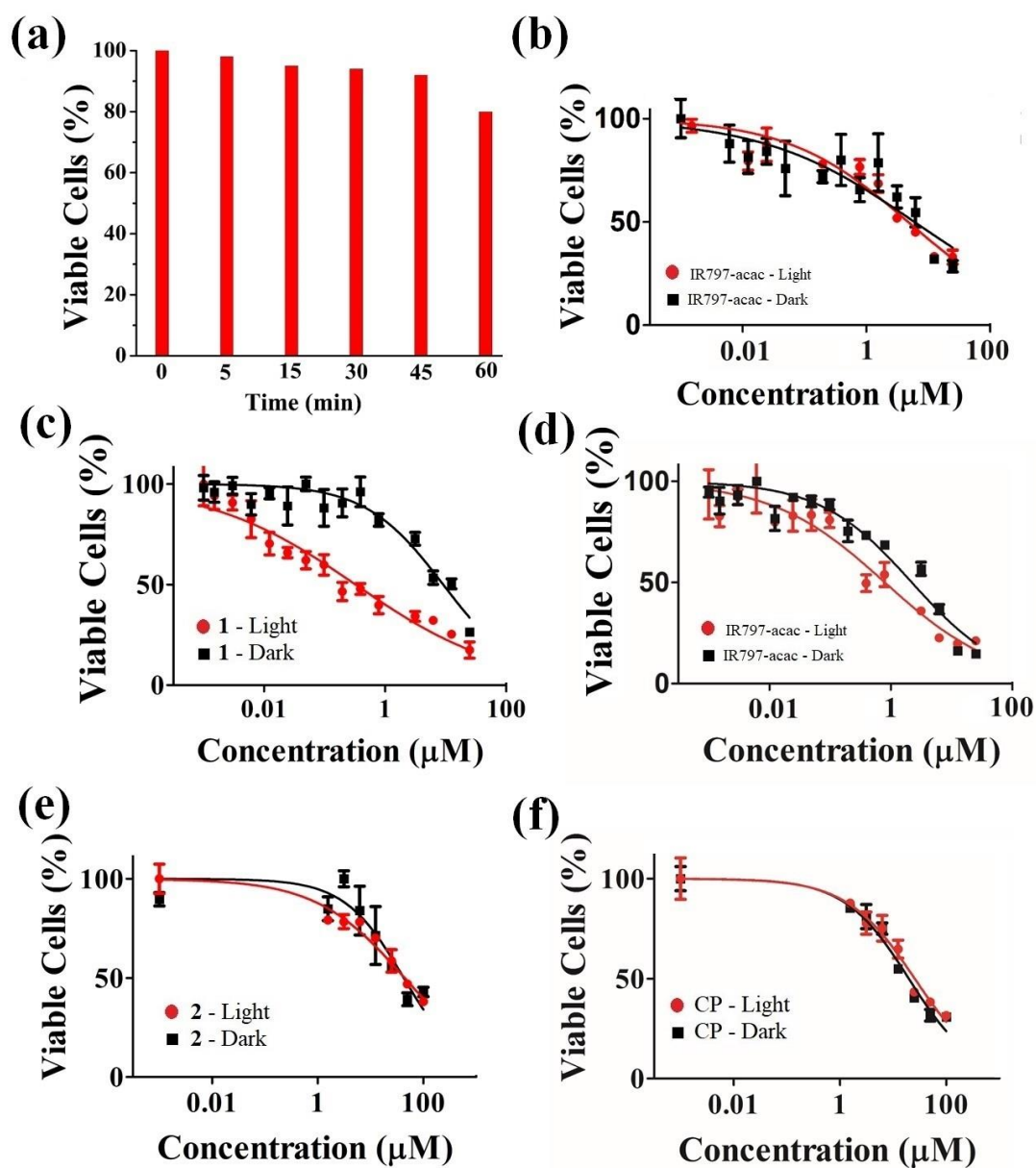


Figure S28. (a) Effect of near-IR light alone on cell viability at different time intervals of irradiation as shown in the graph. (b-f) MTT assays plots depicting concentration dependent changes in percentage cell viabilities of MCF-7 breast cancer cells treated with (b) IR797-acac for 4 h incubation (c) complex **1** for 48 h incubation, (d) IR797-acac for 48 h incubation, (e) complex **2** for 48 h incubation, (f) cisplatin (CP) for 48 h incubation in dark (black squares) and in light (red circles, 720-740 nm, 45 min).

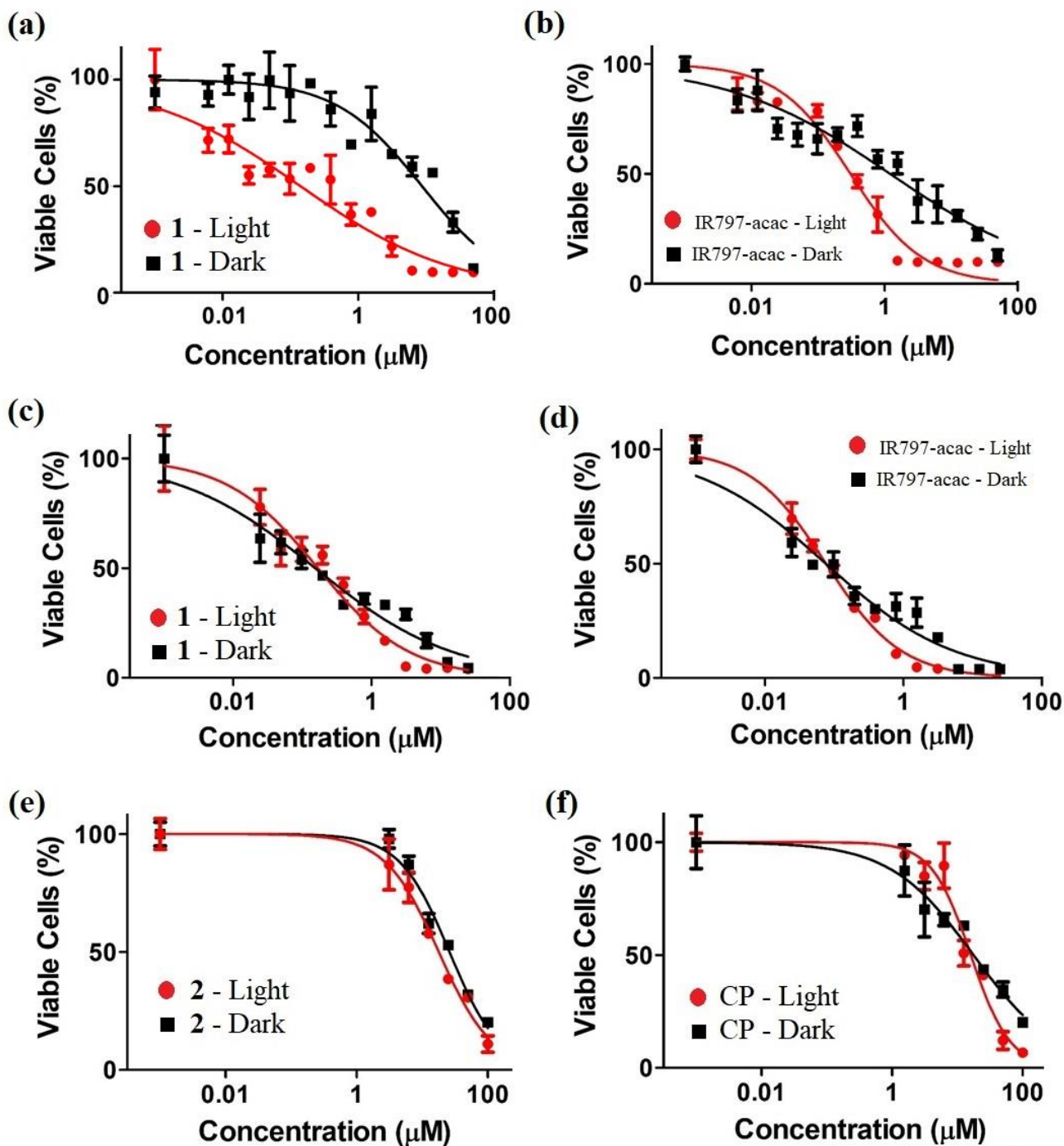


Figure S29. MTT assays plots depicting concentration dependent changes in percentage cell viabilities of C-33 A cervical cancer cells of (a) complex **1** for 4 h incubation (b) IR797-acac for 4 h incubation, (c) complex **1** for 48 h incubation, (d) IR797-acac for 48 h incubation, (e) complex **2** for 48 h incubation and (f) cisplatin (CP) for 48 h incubation in dark (black squares) and in light (red circles, 720-740 nm, 45 min).

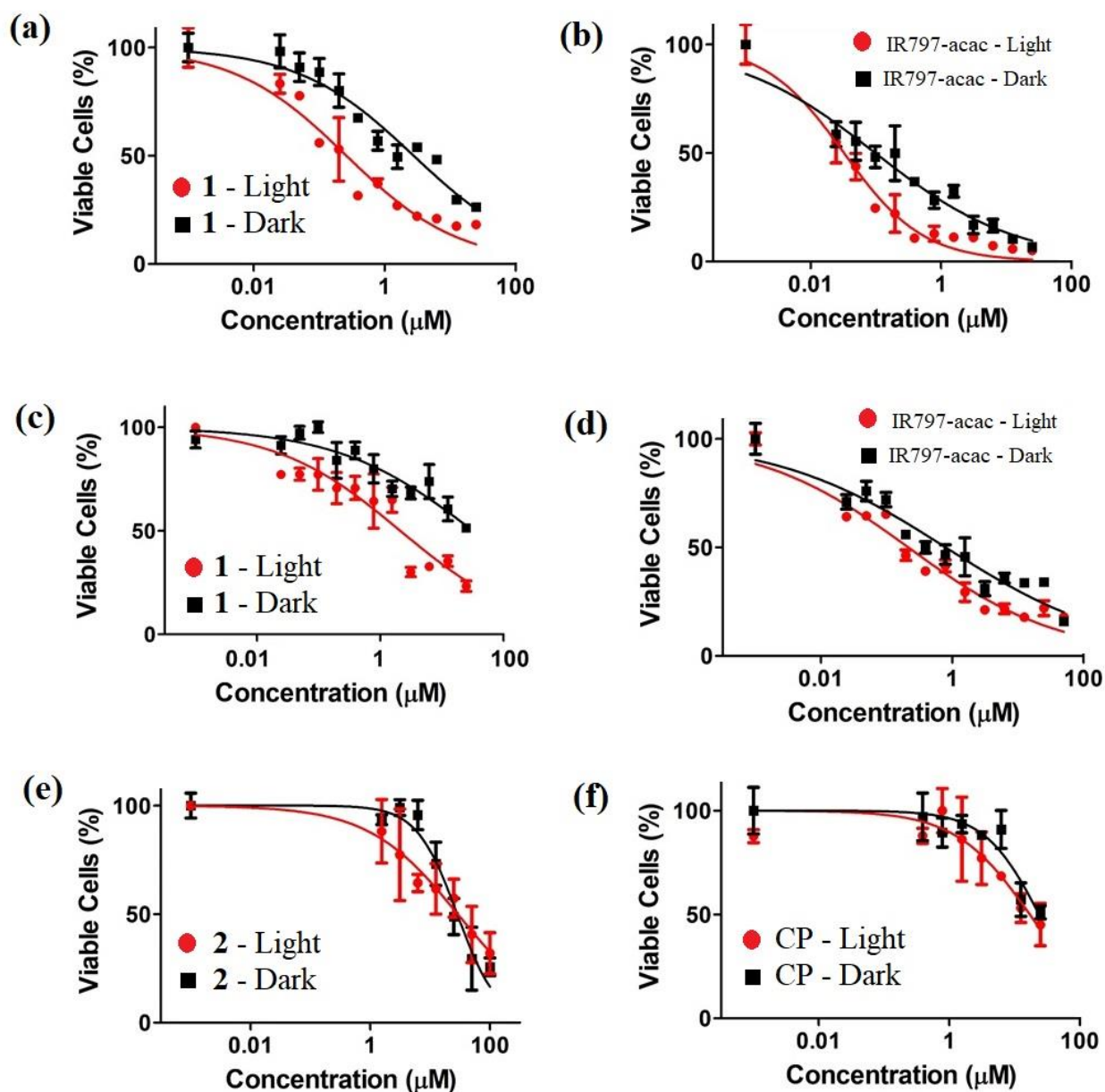


Figure S30. MTT assays plots depicting concentration dependent changes in percentage cell viabilities of HEK293T kidney cells of (a) complex **1** for 4 h incubation (b) IR797-acac for 4 h incubation, (c) complex **1** for 48 h incubation, (d) IR797-acac for 48 h incubation, (e) complex **2** for 48 h incubation and (f) cisplatin (CP) for 48 h incubation in dark (black squares) and in light (red circles, 720-740 nm, 45 min).

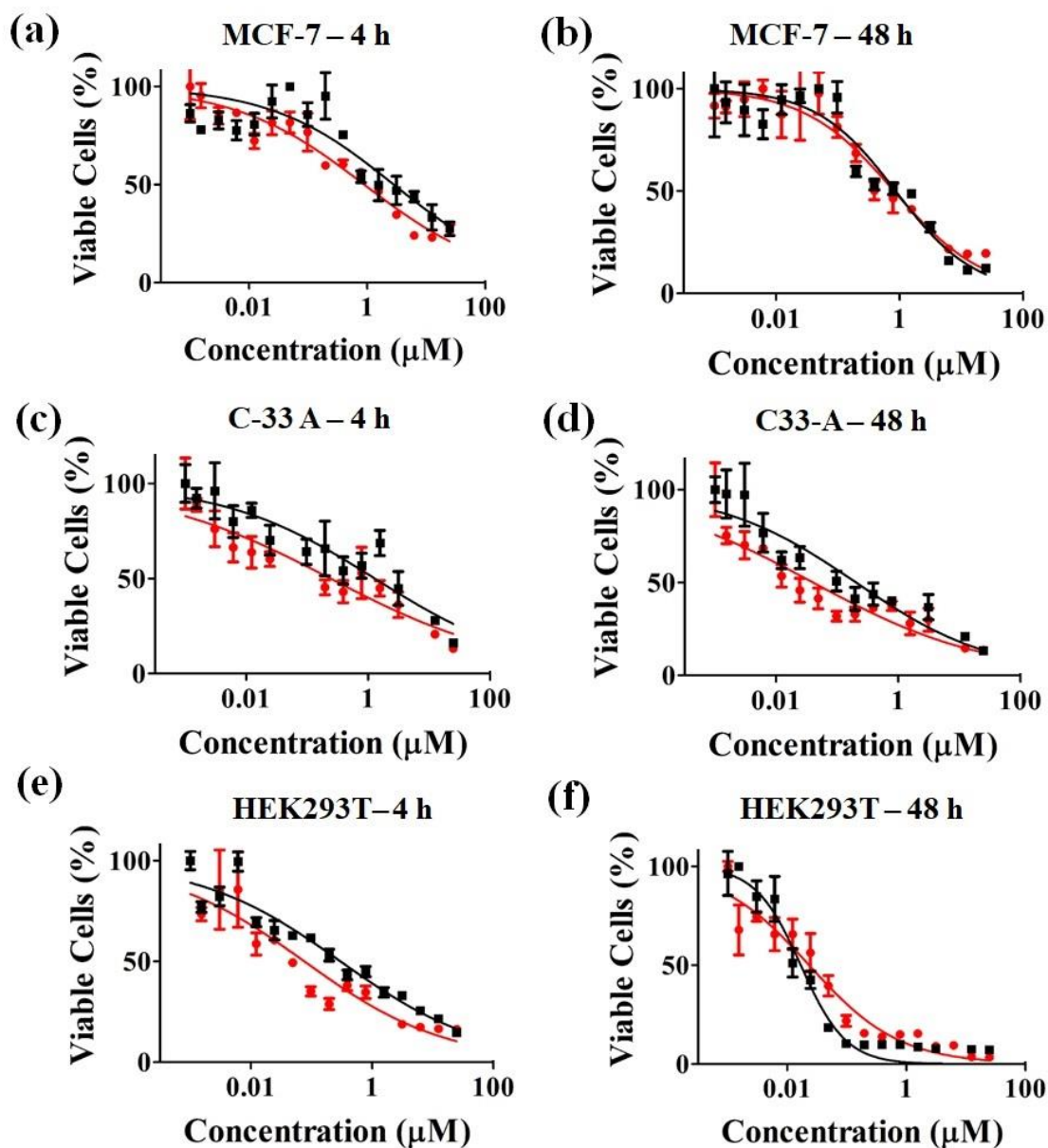


Figure S31. MTT assays plots depicting concentration dependent changes in percentage cell viabilities of different cells lines (as shown in the figure) incubated with an equimolar mixture of IR797acac and cisplatin for 4 h (a, c and e) or 48 h (b, d and f) and either kept in dark (black squares) and irradiated with light (red circles, 720-740 nm, 45 min).

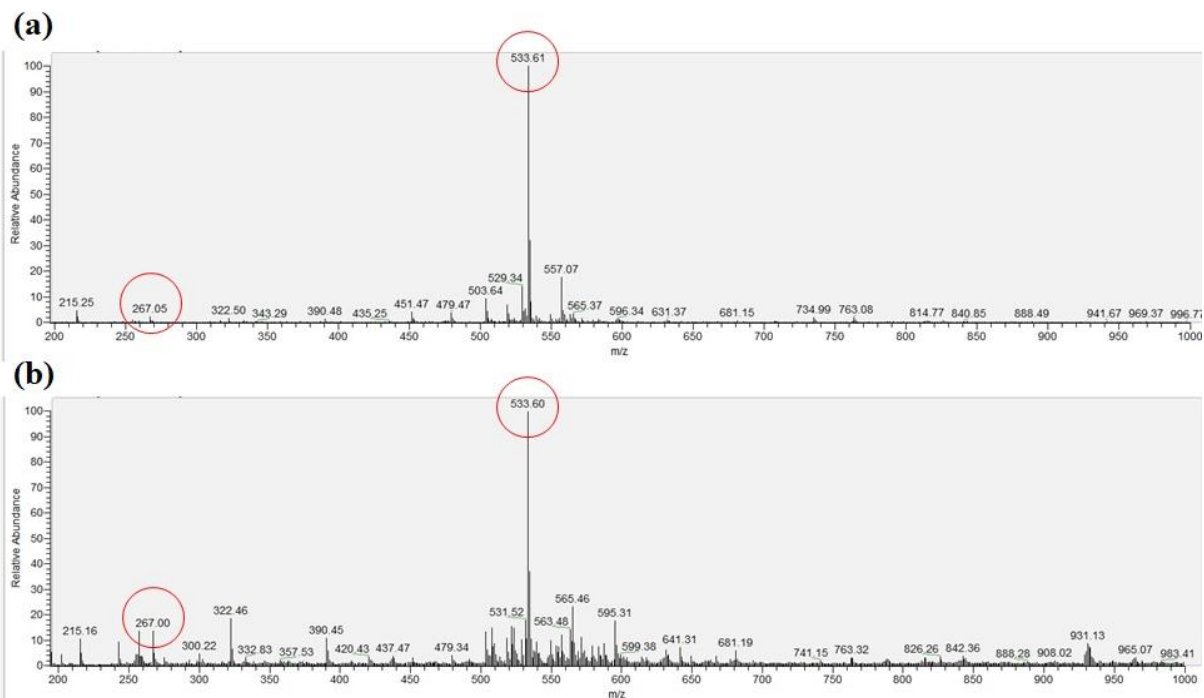


Figure S32. ESI-MS of an equimolar mixture of cisplatin and IR797-acac (diluted in 1:100 ratio from a stock of 25 μM in 0.1% DMSO-PBS) recorded at (a) 0 h and (b) 48 h showing individual peaks (encircled in red) for IR797-acac and cisplatin at 533.6 (expected m/z for $[\text{M}-\text{Cl}]^+ = 533.3$) and 267.0 (expected m/z for $[\text{M}-\text{Cl}]^+$ is 265.5) respectively. The ionizing tendency of IR797-acac is higher than cisplatin and therefore it is appearing as 100% abundant peak and masking all other peaks. These mass spectral studies show that cisplatin and IR797-acac don't react with each other and the combination is stable up to 48 h in dark at pH of 7.4.

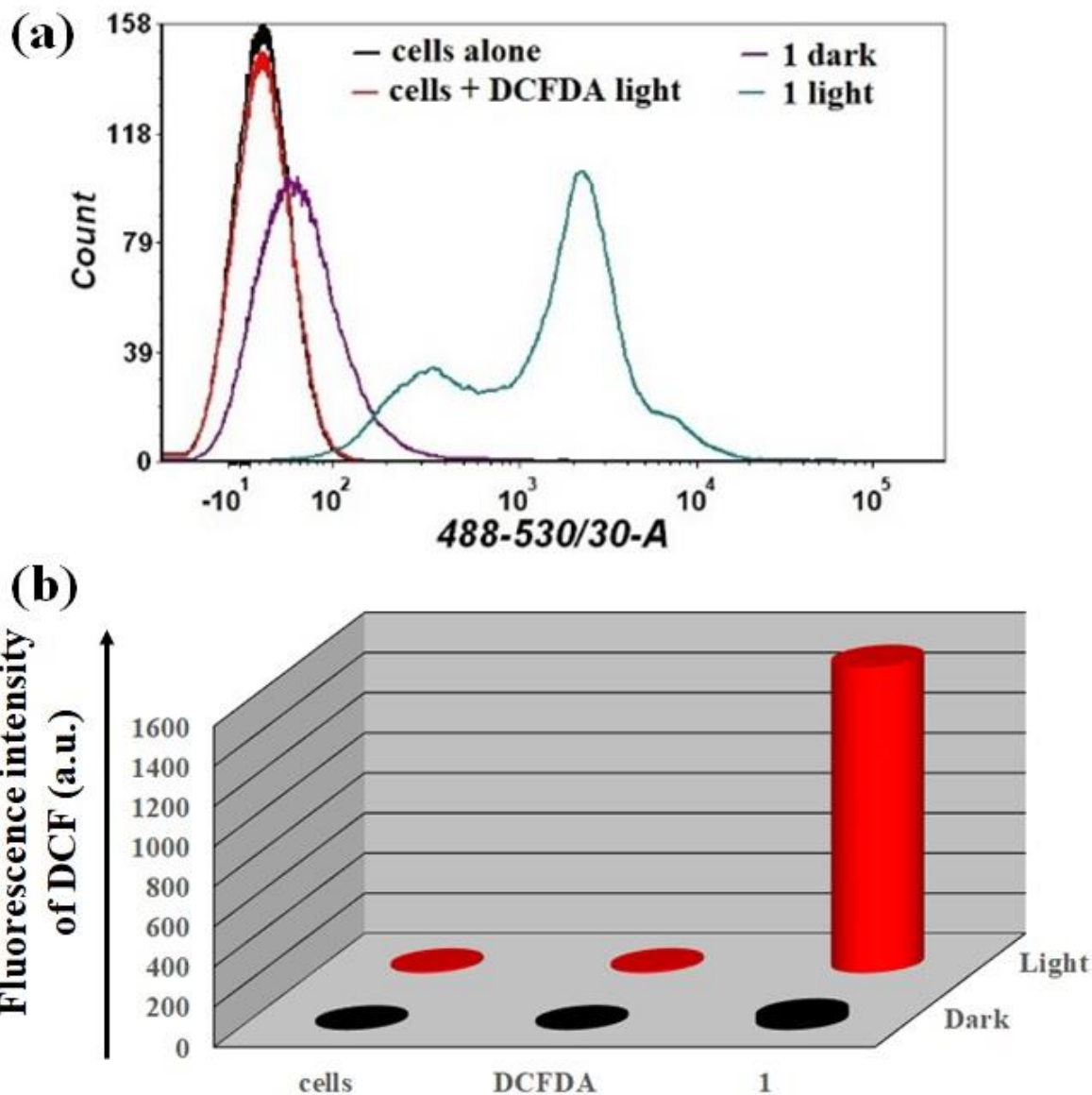


Figure S33. Data obtained from the DCFDA assay represented as (a) histograms and (b) bar diagram for complex **1** ($1 \mu\text{M}$ in 0.05% DMSO-DMEM) performed in C-33 A cells using 4 h incubation in dark and either irradiated with light (720-740 nm, 45 min) or sham-irradiated. Cells alone and cells treated with DCFDA in light and dark conditions were taken as control. Complex **1** shows a right shift of the band which indicates increase in fluorescence intensity of DCF, and hence reactive oxygen species, is generated on light exposure. The bar diagram shows the quantitative results as mean DCF fluorescence intensities. Black cylinders denote experiments in dark and red cylinders denote experiments in near-IR light.

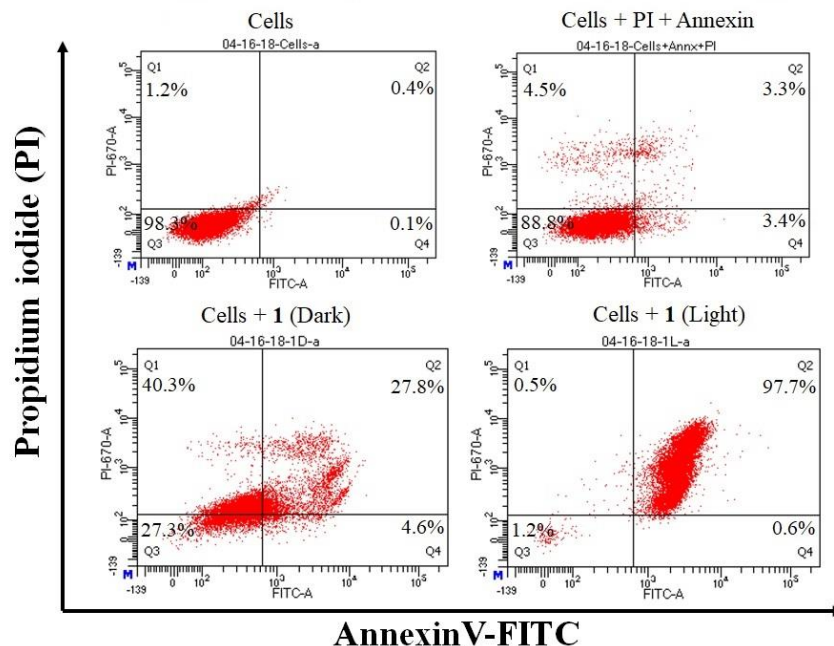


Figure S34. Dot-plots obtained from annexin V-FITC/ PI assay in C-33 A cells showing the percent cell population in each quadrant [Q1, dead cells; Q2, late apoptosis; Q3, live cells; Q4, early apoptosis] of cells alone, cells + PI + annexin, complex **1** (1 μ M in 0.05% DMSO-DMEM) in the dark (4 h) and upon photoexposure (Light, 720-740 nm, 45 min).

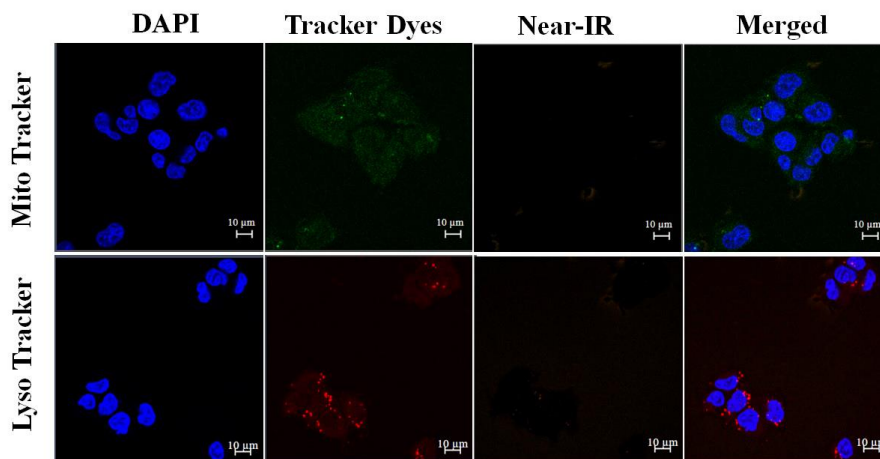


Figure S35. Confocal microscopic images of untreated C-33 A cells showing DAPI (nuclear stain) in first column; tracker dyes (Mito-Tracker® Green, 1st row; Lyso Tracker® Red DND-99, 2nd row) in second column and emission in near-IR channel (no emission detected) in the third column. The last column is an overlapped image of the first three columns. Scale bar = 10 μ m.

Table S1. Spectroscopic data for complex **1** and IR797-acac

Compound	λ_{abs} (nm)	λ_{em}	$[\phi_f]^b$	$t_{1/2}^D$	$t_{1/2}^L$	ϕ_{Δ}
	$[\epsilon \times 10^{-4} (\text{M}^{-1} \cdot \text{cm}^{-1})]^a$	(nm) ^a	$[\tau_f (\text{ps})]^c$	(h) ^d	(sec) ^d	$[t_{1/2}^{\text{DPBF}} (\text{sec})]^e$
1	790 [4.5], 715 [1.6], 445 [0.3]	820	0.32 [31.75]	20	120	0.15 [30]
IR797-acac	785 [5.0], 707 [2.4], 445 [0.16]	825	0.53 [27.10]	10	40	0.017 [360]

^aAbsorption and emission studies are carried out in 0.1% DMSO-PBS (pH = 7.4). Excitation wavelength used for emission is 780 nm. ^bQuantum yields of fluorescence in DMSO [indocyanine green (ICG) as standard, $\phi_f = 0.13$ in DMSO].^[S8] Data has ± 10 % deviations. ^cExcited state lifetimes in 50% DMSO-PBS solutions (excitation = 740 nm, emission = 810 nm). ^dStability studies are done in 0.5% DMSO in 10% FBS-DMEM solutions. ^eQuantum yield of singlet oxygen generation in DMF [methylene blue as standard, $\phi_f = 0.52$].^[S3d] Data has ± 10 % deviations. LED light source of 720-740 nm is used for the experiments with light exposure. L denotes experiments carried out in light and D is for the same experiments done in absence of light.

Table S2. Amount of Pt (ng/ μM ct-DNA) as estimated from ICP-MS^a

Complex	Time intervals (h)							
	0.25		0.5		1		24	
	Light	Dark	Light	Dark	Light	Dark	Light	Dark
1	2.3 \pm 0.5	0.9 \pm 0.2	7.1 \pm 0.8	1.7 \pm 0.2	7.8 \pm 1.1	3.9 \pm 1.2	13.5 \pm 2.1	12.9 \pm 2.4
2	n.d.	n.d.	n.d.	n.d.	n.d.	n.d.	n.d.	22.6 \pm 3.2
cisplatin	n.d.	n.d.	n.d.	n.d.	n.d.	n.d.	n.d.	40.1 \pm 5.5

^aCalf-thymus DNA (ctDNA, 500 μM) treated with complex **1**, **2** or cisplatin (50 μM) in 0.5% DMSO-PBS (pH = 7.4). Samples were either non-irradiated (dark) or irradiated (light) using LED light source of wavelength 720-740 nm for the time interval of 15 min, 30 min, 1 h and 24 h. n.d. denotes “not determined”.

Table S3. Energy-minimized structure of complex **1** by DFT methods using B3LYP/(LANL2DZ for Pt and 6-31+G for other atoms)

Atoms	X	Y	Z
6	-0.283750888	0.274410618	-0.584354291
8	-1.088600820	-1.749458144	-1.715033724
6	-0.607955808	-0.515826921	-1.733383660
6	-0.276383483	-0.228526573	0.751604359
8	-0.684040950	-1.433511512	1.128776306
6	0.172463187	1.688456151	-0.829413095
6	1.533613946	2.088756383	-0.700878068
6	1.672966604	3.572688067	-1.015966183
6	0.321360479	3.939428073	-1.683563622
6	-0.608526309	2.748490152	-1.397330098
6	2.621206476	1.242917097	-0.397866659
6	3.939845377	1.713837683	-0.235781581
6	-1.898067726	2.784156905	-1.968428033
6	-3.145848761	2.118952506	-1.805945492
6	-5.749056988	2.160877960	2.613463761
6	-5.198379976	1.957847536	1.345270068
6	-5.899216060	1.197831164	0.390082634
6	-7.155735107	0.634688123	0.650435877
6	-7.705245834	0.847574357	1.932152863
6	-7.012215993	1.598128908	2.904655110
6	-3.889434232	2.463018733	0.739927158
6	-3.936392575	1.836256378	-0.678045641
7	-5.116610042	1.132900110	-0.802248516
6	-2.676846601	2.021247415	1.590257259
6	-3.910136393	4.017750031	0.613370588
6	-5.569646004	0.460805379	-2.023872833
6	8.758613788	0.598009625	0.973945102
6	7.411740265	0.606054897	0.602916474
6	6.749251520	-0.608539549	0.345190174
6	7.382795699	-1.852612247	0.454360971
6	8.742023605	-1.851425017	0.830908459
6	9.423833724	-0.643414642	1.086515634
6	6.441853038	1.764303433	0.402956404
6	5.141151156	1.022607908	0.020989575
7	5.390595230	-0.321144894	-0.025305385
6	4.467981417	-1.367138096	-0.478209113
6	6.903906481	2.698269570	-0.757225417
6	6.253786195	2.586456401	1.711375876
6	0.260844155	0.551648999	1.932197971
6	-0.396834624	-0.019608157	-3.145556782
78	-1.427391832	-2.847889219	-0.075483212
7	-2.152889114	-4.271753582	-1.431133580
7	-1.712847767	-3.914169284	1.704690796

SUPPORTING INFORMATION

Table S4. Electronic transitions of complex **1** in the red and near-IR region as predicted by TDDFT using functional B3LYP/ (LANL2DZ for Pt and 6-31+G for other atoms)

Energy (eV)	Excited State	λ (nm)	Oscillator strength (<i>f</i>)	Orbitals involved (% contribution)	Nature of transition
1.5891	Singlet	780.23	0.0755	HOMO \rightarrow LUMO + 1 (82) HOMO \rightarrow LUMO (18)	LMCT
1.6072	Triplet	771.41	0.0000	HOMO \rightarrow LUMO + 1 (100)	LMCT
1.7885	Triplet	692.83	0.0000	HOMO \rightarrow LUMO (97) HOMO - 5 \rightarrow LUMO (3)	ILCT
1.9169	Singlet	646.81	1.3866	HOMO \rightarrow LUMO (78) HOMO \rightarrow LUMO + 1 (17) HOMO \leftarrow LUMO (5)	ILCT

LMCT = Ligand (cyanine) to metal (Pt(II)) charge transfer. ILCT = Intraligand charge transfer.

SUPPORTING INFORMATION

Table S5. Bond lengths (Å), bond angles (°) and Mulliken atomic charges of the coordination sphere of complex **1** optimized by B3LYP/LanL2DZ (for Pt atom)/6-31+G (for all other atoms) functionals

Parameters		Ground state geometry	Excited triplet state geometry
Bond Lengths	Pt – O1	2.002	2.157
	Pt – O2	2.008	2.167
	Pt – N1	2.095	2.271
	Pt – N2	2.094	2.265
Bond Angles	N1 – Pt – N2	99.017	109.137
	O1 – Pt – O2	92.418	85.182
	N1 – Pt – O1	84.204	82.421
	N2 – Pt – O2	84.354	83.265
Mulliken atomic charges	Pt	0.738497	0.361226
	O1	-0.535053	-0.378438
	O2	-0.479282	-0.387366
	N1	-0.869836	-0.859384
	N2	-0.893155	-0.856727

SUPPORTING INFORMATION

Table S6. Singlet transitions of dioxetane intermediates P1a and P1b in the visible region as predicted by TDDFT calculations

Compound	Energy (eV)	λ (nm)	Oscillator strength (<i>f</i>)	Orbitals involved (% contribution)
P1a	1.9571	633.50	0.0157	HOMO – 1 \rightarrow LUMO (79)
	2.0832	595.17	0.0536	HOMO – 3 \rightarrow LUMO (37) HOMO – 2 \rightarrow LUMO (42)
	2.1568	574.86	0.1716	HOMO – 4 \rightarrow LUMO (52) HOMO – 3 \rightarrow LUMO (27)
	2.5905	478.62	0.8327	HOMO – 4 \rightarrow LUMO (40) HOMO – 2 \rightarrow LUMO (26)
	2.8494	435.12	0.2500	HOMO – 5 \rightarrow LUMO (89)
P1b	1.7180	721.67	0.0042	HOMO – 2 \rightarrow LUMO (86)
	1.9777	626.93	0.0001	HOMO – 1 \rightarrow LUMO (86)
	2.3332	531.40	0.0005	HOMO – 3 \rightarrow LUMO (97)
	2.3757	521.89	0.2959	HOMO – 4 \rightarrow LUMO (70)
	2.4271	510.83	0.0014	HOMO \rightarrow LUMO + 1 (100)
	2.6626	465.65	0.2641	HOMO – 5 \rightarrow LUMO (85)

SUPPORTING INFORMATION

Table S7. IC₅₀ values (μM) in different cell lines as obtained from MTT assay^a

Cells→ Comp↓	MCF-7		C-33 A		HEK293T	
	Light ^b	Dark ^c	Light ^b	Dark ^c	Light ^b	Dark ^c
1	0.32 ± 0.10 (0.65 ± 0.23)	9.1 ± 1.1 (18.2 ± 3.2)	0.17 ± 0.09 (0.14 ± 0.05)	0.15 ± 0.05 (8.4 ± 1.4)	0.26 ± 0.08 (2.10 ± 0.50)	2.8 ± 1.9 (15.1 ± 4.8)
2	44.2 ± 5.1	42.6 ± 4.7	18.5 ± 2.4	25.1 ± 3.1	28.5 ± 2.2	29.1 ± 3.4
IR797-acac	0.95 ± 0.32 (4.7 ± 0.8)	1.5 ± 0.3 (5.9 ± 0.3)	0.07 ± 0.01 (0.30 ± 0.7)	0.07 ± 0.01 (1.2 ± 0.1)	0.03 ± 0.01 (0.21 ± 0.03)	1.1 ± 0.02 (2.84 ± 0.20)
Cisplatin (CP)	22.5 ± 3.2	25.0 ± 2.2	16.1 ± 1.5	17.7 ± 1.5	17.1 ± 2.2	23.8 ± 4.1
IR797-acac + CP ^d	0.81 ± 0.24 (0.88 ± 0.17)	0.88 ± 0.18 (2.6 ± 1.4)	0.05 ± 0.14 (0.25 ± 0.15)	0.09 ± 0.22 (1.4 ± 0.8)	0.01 ± 0.005 (0.10 ± 0.04)	0.02 ± 0.007 (0.30 ± 0.11)

^aCells incubated with compounds for either 48 h (or 4 h in parenthesis) in dark. ^bIrradiated with light of 720-740 nm for 45 min in phenol-red free media. ^cIn dark. ^dCells incubated with an equimolar mixture of cisplatin (CP) and IR797-acac.

Table S8. Cellular uptake (ng of Pt/ 10⁶ cells) in C-33 A cells as quantified by ICP-MS^a

Compound	Whole Cell	Nuclear	Cytoplasmic
1 (light) ^b	100	67	22
1 (dark) ^c	195	41	138
2	80	14	46
Cisplatin	59	13	43

^aCells treated with complex **1**, **2** or cisplatin in dark for 4 h (C-33 A) and quantified for platinum uptake in whole cell, cytoplasmic and nuclear fractions by ICP-MS measurements. ^b Irradiated with light of 720-740 nm for 15 min in phenol-red free media. ^c In dark. Deviations are within ± 10%.

SUPPORTING INFORMATION

References

- [S1] J. J. Wilson, S. J. Lippard, *J. Med. Chem.* **2012**, *55*, 5326-5336.
- [S2] S. U. Dunham, H. T. Chifotides, S. Mikulski, A. E. Burr, K. R. Dunbar, *Biochem.* **2005**, *44*, 996-1003.
- [S3] a) I. Carmichael, G. L. Hug, *J. Phys. Chem. Ref. Data* **1986**, *15*, 1; b) W. Li, L. Li, H. Xiao, R. Qi, Y. Huang, Z. Xie, X. Jing, H. Zhang, *RSC Adv.* **2013**, *3*, 13417-13421. c) N. Adarsh, R. R. Avirah, D. Ramaiah, *Org. Lett.* **2010**, *12*, 5720-5723. d) R. W. Redmond, J. N. Gamlin, *Photochem. Photobiol.* **1999**, *70*, 391-475.
- [S4] a) M. J. Frisch, G. W. Trucks, H. B. Schlegel, G. E. Scuseria, M. A. Robb, J. R. Cheeseman, G. Scalmani, V. Barone, B. Mennucci, G. A. Petersson, H. Nakatsuji, M. Caricato, X. Li, H. P. Hratchian, A. F. Izmaylov, J. Bloino, G. Zheng, J. L. Sonnenberg, M. Hada, M. Ehara, K. Toyota, R. Fukuda, J. Hasegawa, M. Ishida, T. Nakajima, Y. Honda, O. Kitao, H. Nakai, T. Vreven, J. A. Montgomery Jr., J. E. Peralta, F. Ogliaro, M. Bearpark, J. J. Heyd, E. Brothers, K. N. Kudin, V. N. Staroverov, R. Kobayashi, J. Normand, K. Raghavachari, A. Rendell, J. C. Burant, S. S. Iyengar, J. Tomasi, M. Cossi, N. Rega, J. M. Millam, M. Klene, J. E. Knox, J. B. Cross, V. Bakken, C. Adamo, J. Jaramillo, R. Gomperts, R. E. Stratmann, O. Yazyev, A. J. Austin, R. Cammi, C. Pomelli, J. W. Ochterski, R. L. Martin, K. Morokuma, V. G. Zakrzewski, G. A. Voth, P. Salvador, J. J. Dannenberg, S. Dapprich, A. D. Daniels, Ö. Farkas, J. B. Foresman, J. V. Ortiz, J. Cioslowski and D. J. Fox, *GAUSSIAN 09 (Revision A.1)*, Gaussian, Inc., Wallingford, CT, **2009**; b) A. D. Becke, *Phys. Rev. A* **1988**, *38*, 3098-3100; c) A. D. Becke, *J. Chem. Phys.* **1993**, *98*, 5648-5652; (d) C. Lee, W. Yang, R. G. Parr, *Phys. Rev. B: Condens. Matter* **1988**, *37*, 785-789.
- [S5] T. Mosmann, *J. Immunol. Methods* **1983**, *65*, 55– 63.
- [S6] M. Price, D. Kessel, *J. Biomed. Opt.* **2010**, *15*, 0516051.
- [S7] I. Vermes, C. Haanen, H. Stefens-Nakken, C. Reutelingsperger, *J. Immunol. Methods* **1995**, *184*, 39– 51.
- [S8] C. Li, T. R. Greenwood, Z. M. Bhujwalla, K. Glunde, *Org. Lett.* **2006**, *8*, 3623-3626.